

Higher multipoles of the galaxy bispectrum in redshift space

Yue Nan,^a Kazuhiro Yamamoto,^a Chiaki Hikage^b

^aDepartment of Physics, Graduate School of Physical Sciences, Hiroshima University, Higashi-Hiroshima, Kagamiyama 1-3-1, 739-8526, Japan

^bKavli Institute for the Physics and Mathematics of the Universe (Kavli IPMU, WPI), The University of Tokyo, 5-1-5 Kashiwanoha, Kashiwa, Chiba, 277-8583, Japan

Abstract. As a generalization of our previous work [Phys. Rev. D 95 043528 (2017)], in which an analytic model for the galaxy bispectrum in redshift space was developed on the basis of the halo approach, we here investigate its higher multipoles that have not been known so far. The redshift-space bispectrum includes the two variables ω and ϕ for the line-of-sight direction, and the higher multipole bispectra are defined by the coefficients in the expansion of the redshift-space bispectrum using the spherical harmonics. We find 6 new nonvanishing components out of 25 total components up to $\ell = 4$, in addition to 3 components discussed in the previous work (monopole, quadrupole, and hexadecapole of $m = 0$). The characteristic behaviors of the new nonvanishing multipoles are compared with the results of galaxy mock catalogs that match the halo occupation distribution of the Sloan Digital Sky Survey Baryonic Oscillation Spectroscopic Survey low-redshift sample. We find that the multipoles with $m \neq 0$ are also sensitive to redshift-space distortion (RSD) as well as those with $m = 0$ and thus are key ingredients in the RSD analysis using the galaxy bispectrum. Analytic approximation formulas for these nonzero components are also presented; these are useful for understanding the characteristic behaviors.

Keywords: Large scale structure of the Universe, power spectrum

Contents

1	Introduction	1
2	Basis for bispectrum in redshift space	2
2.1	Halo model	2
2.2	Bispectrum in redshift space	4
3	Multipole bispectrum	6
3.1	Definition of multipole bispectrum	6
3.2	Results	8
3.3	Comparison with the results of mock catalogs	10
4	Discussion: approximate formulas	10
5	Summary and Conclusions	11
A	Spherical Harmonics	13
B	Approximate formulas	13

1 Introduction

In statistical analysis of the large-scale structure of galaxies, the basic quantities are the two-point correlation function and the power spectrum which are related by the Fourier transformation. If the fluctuations are statistically isotropic and Gaussian, the monopole power spectrum should be enough to characterize the statistical properties. However, non-Gaussian properties might have been imprinted in the initial conditions of primordial fluctuations [1]. Furthermore, in the course of evolution of cosmic structure formation, the non-Gaussian properties are generated in the density perturbation and in the galaxy distributions owing to the nonlinearity of gravitational clustering and structure formation (e.g., [2–5]). The three-point correlation function in the configuration space and its Fourier transformation, i.e., the bispectrum, is the lowest order statistical quantity used to characterize these non-Gaussian properties (see, e.g., [6] for a review) The first measurements of the three-point correlation function were reported in Refs. [7, 8], thereafter many works have been carried out [9–26]. On the other hand, the measurement of the bispectrum was carried out for the first time by Fry and Seldner [27], and it was advanced as in the Refs. [28–34].

In the analysis of the higher order statistics with galaxy catalogs of redshift surveys, peculiar velocities of galaxies break the assumption of statistical isotropy in the distribution in redshift space through redshift-space distortion. On large scales, the linear velocity field induces a linear redshift-space distortion [35, 36]; however, on small scales, the random velocity of galaxies make a significant contribution to the distribution in redshift space, which is called the Finger of God (FoG) effect [37, 38]. The redshift-space distortion generates the additional non-Gaussianity in the galaxy distribution in redshift space [39]. Especially, the FoG effect is the cause of the non-Gaussianity on small scales, reflecting the nonlinear evolution of the cosmic structure formation as well. Recently, higher multipoles which characterize

the redshift space-distortions in the three-point correlation function and the bispectrum are discussed [26, 33, 34, 40, 41].

In the present paper, we focus on the galaxy bispectrum in redshift space. A precise theoretical model is necessary to obtain cosmological information beyond the two point statistics from the galaxy bispectrum [42–51] Recently, various general relativistic effects and the wide angle effect in the bispectrum are also discussed [52–58]. However, the bispectrum is quite complicated even in the simplest case within the general relativity. Therefore, an analytic model that reproduces their behaviors well is quite useful. The halo approach is useful to find such a theoretical model that is applicable from large to small scales [59–62]. The theoretical framework, based on the assumption that all the dark matter and galaxies are associated with virialized dark matter halos, is characterized by the halo density profile $\rho(r)$, the halo mass function dn/dM , and the halo's correlation, where $\rho(r)$ represents the density of each halo and dn/dM represents the number density of halos with mass M . In Ref. [63], the authors developed a theoretical model to explain the multipole power spectra in redshift space of the Sloan Digital Sky Survey (SDSS) luminous red galaxies (LRGs) on the basis of the halo approach, in which the halo occupation distribution (HOD) of the central galaxy and satellite galaxies plays an important role. The theoretical model well reproduces the results of the observational data. In our previous paper [40], the theoretical approach was applied to the model for the galaxy bispectrum in redshift space. We demonstrated that the theoretical model reproduces the behaviors of the bispectrum of mock galaxy catalogs of the low-redshift (LOWZ) galaxy sample of the SDSS III Baryon Oscillation Spectroscopic Survey (BOSS) survey [64]. An advantage of the theoretical approach is that analytic approximate expressions for the bispectrum can be obtained, which is useful for understanding how the bispectrum depends on the parameters qualitatively.

As a generalization of the previous work [40], we investigate higher multipoles of the bispectrum. We find the nonvanishing higher multipole components of the bispectrum, which have not been known so far. Such components of the bispectrum will be useful for characterizing the unique non-Gaussian properties of the galaxy distribution in redshift space. This paper is organized as follows. In Section 2, we introduce the multipoles of the bispectrum as coefficients in the multipole expansion with respect to the spherical harmonics $Y_{\ell,m}(\omega, \phi)$, where ω and ϕ are the parameters for the line-of-sight direction. Previous works only investigated the components of $m = 0$ [39–41]. We find six new components of real functions up to $\ell = 4$. In Section 3, the behaviors of the new multipoles of the bispectrum are demonstrated by adopting the HOD of the SDSS III BOSS LOWZ sample. In Section 4, the properties of the multipoles of the bispectrum are investigated in an analytic way. Section 5 is devoted to a summary and conclusions. Appendix A lists the expression for the spherical harmonics. Appendix B lists the analytic formulas for the multipoles of the bispectrum in redshift space. In the present paper, we adopt a spatially flat cold dark matter (CDM) cosmology with a cosmological constant Λ adopting the parameters $\Omega_b = 0.046$, $\Omega_m = 0.273$, $n_s = 0.963$, $h = 0.704$, $\tau = 0.089$, and $\sigma_8 = 0.809$.

2 Basis for bispectrum in redshift space

2.1 Halo model

We first introduce the bispectrum in redshift space in the halo approach. The halo approach is quite useful for characterizing the distributions of dark matter as well as the distributions of galaxies, from large scales to smaller scales, where nonlinearity plays an important role

[59–63, 65]. In the present paper, we follow the theoretical model developed in Ref. [40], where an analytic expression was presented for the bispectrum in which the halo approach was applied, with the HOD description of central galaxies and satellite galaxies. By adopting the model of [40], a generalized model will be developed.

As addressed previously, the basic quantities used in the halo approach are the halo density profile $\rho(r)$ characterizing the matter distribution within halos and the halo mass function dn/dM describing the distribution of halos themselves. In addition, random motions of galaxies within halos, as an embodiment of nonlinearity on small scales, are characterized by assuming an uncorrelated one-dimensional velocity dispersion yielding a Gaussian distribution. The HOD offers a method for linking statistical quantities of galaxies to that of halos in the halo approach.

For the halo density profile $\rho(r)$, assuming the truncated Navarro–Frenk–White (NFW) density profile [66] of dark matter, we can write

$$\rho(r) = \begin{cases} \frac{\rho_s}{r/r_s(1+r/r_s)^2} & (r < r_{\text{vir}}), \\ 0 & (r > r_{\text{vir}}), \end{cases} \quad (2.1)$$

where ρ_s and r_s are the parameters representing the characteristic density and the characteristic scale, and r_{vir} is the virial radius, which determines the virial mass of a halo by $M_{\text{vir}} = 4\pi \int_0^{r_{\text{vir}}} dr r^2 \rho(r) = 4\pi r_{\text{vir}}^3 \Delta_{\text{vir}} \bar{\rho}_m(z)/3$, where $\bar{\rho}_m(z)$ is the mean matter density and we adopt the value $\Delta_{\text{vir}} = 265$ at redshift $z = 0.3$. Because our interest is focused on the quantity in Fourier space, we denote the Fourier transform of $\rho(r)$ by

$$\tilde{u}_{\text{NFW}}(k; M) = \frac{\int_{r \leq r_{\text{vir}}} d^3x \rho(r) e^{-ik \cdot x}}{\int_{r \leq r_{\text{vir}}} d^3x \rho(r)}. \quad (2.2)$$

For the distribution of halos, we adopt the fitting formula in Refs. [67–69] for the halo mass function in the form

$$M \frac{dn}{dM} = \frac{\bar{\rho}_m}{M} \frac{d \ln \sigma_R^{-1}}{d \ln M} f(\sigma_R) \quad (2.3)$$

with

$$f(\sigma_R) = 0.322 \sqrt{\frac{2 \times 0.707}{\pi}} \left[1 + \left(\frac{1}{0.707\nu^2} \right)^{0.3} \right] \nu \exp \left(-\frac{0.707\nu^2}{2} \right) \quad (2.4)$$

and $\nu = \delta_c/\sigma_R$, where σ_R is the root-mean-square fluctuation in spheres containing mass M at the initial time, extrapolated to redshift z using linear theory, and $\delta_c (\simeq 1.686)$ is the critical value of the initial overdensity that is required for gravitational collapse.

We assume that the distribution of satellite galaxies follows the NFW profile and that the satellite galaxies have internal random velocities following a Gaussian distribution specified by the one-dimensional velocity dispersion [63, 70–72],

$$\sigma_{v,\text{off}}(M) = \left(\frac{GM}{2r_{\text{vir}}} \right)^{1/2}. \quad (2.5)$$

These random motions cause the FoG effect, which changes the distribution of satellite galaxies in redshift space. If satellite motions in a halo are uncorrelated with each other, then the Fourier transform of the distribution of the satellite galaxies in redshift space yields

$$\tilde{u}(\mathbf{k}, M) = \tilde{u}_{\text{NFW}}(k; M) \exp \left[-\frac{\sigma_{v,\text{off}}^2(M) k^2 \mu^2}{2a^2 H^2(z)} \right], \quad (2.6)$$

where $H(z)$ is the Hubble parameter at the redshift z .

To link the distribution of satellite galaxies in redshift space to that of halos, we introduce the halo occupation distribution $N_{\text{HOD}}(M)$, which describes the average occupation number of galaxies inside a halo with mass M . We adopt the following fitting formula for central galaxies and satellite galaxies [73]:

$$N_{\text{HOD}}(M) = \langle N_c \rangle (1 + \langle N_s \rangle), \quad (2.7)$$

$$\langle N_c \rangle = \frac{1}{2} \left[1 + \text{erf} \left(\frac{\log_{10}(M) - \log_{10}(M_{\min})}{\sigma_{\log M}} \right) \right], \quad (2.8)$$

$$\langle N_s \rangle = \left(\frac{M - M_{\text{cut}}}{M_1} \right)^{\alpha}, \quad (2.9)$$

where $\text{erf}(x)$ is the error function. For specific values, the HOD parameters are listed in Table I for the SDSS-III BOSS LOWZ catalog [64].

2.2 Bispectrum in redshift space

If we denote the galaxy number density contrast by $\delta(t, \mathbf{k})$, the bispectrum $B_g(t, \mathbf{k}_1, \mathbf{k}_2, \mathbf{k}_3)$ is defined by

$$\langle \delta(t, \mathbf{k}_1) \delta(t, \mathbf{k}_2) \delta(t, \mathbf{k}_3) \rangle = (2\pi)^3 \delta_D^{(3)}(\mathbf{k}_1 + \mathbf{k}_2 + \mathbf{k}_3) B_g(t, \mathbf{k}_1, \mathbf{k}_2, \mathbf{k}_3). \quad (2.10)$$

Thus the bispectrum $B_g(t, \mathbf{k}_1, \mathbf{k}_2, \mathbf{k}_3)$ relies on the implicit assumption $\mathbf{k}_1 + \mathbf{k}_2 + \mathbf{k}_3 = 0$. This means that the bispectrum is described by the five parameters $k_1, k_2, \cos \theta_{12} (= \mathbf{k}_1 \cdot \mathbf{k}_2 / k_1 k_2)$, $\mu (= \cos \omega)$, and ϕ as variables, with which we may write the vectors

$$\mathbf{k}_1 = (0, 0, k_1), \quad (2.11)$$

$$\mathbf{k}_2 = (0, k_2 \sin \theta_{12}, k_2 \cos \theta_{12}), \quad (2.12)$$

$$\mathbf{k}_3 = (0, -k_2 \sin \theta_{12}, -k_1 - k_2 \cos \theta_{12}), \quad (2.13)$$

$$\boldsymbol{\gamma} = (\sin \omega \cos \phi, \sin \omega \sin \phi, \cos \omega), \quad (2.14)$$

where $\boldsymbol{\gamma}$ denotes the unit vector of the line of sight direction. Figure 1 shows the configuration of the variables. Then, we define μ_i as

$$\mu_1 = \hat{\mathbf{k}}_1 \cdot \boldsymbol{\gamma} = \cos \omega = \mu, \quad (2.15)$$

$$\mu_2 = \hat{\mathbf{k}}_2 \cdot \boldsymbol{\gamma} = \sin \theta_{12} \sin \omega \sin \phi + \cos \theta_{12} \cos \omega = \sin \theta_{12} \sqrt{1 - \mu^2} \sin \phi + \cos \theta_{12} \mu, \quad (2.16)$$

$$\mu_3 = -\frac{k_1}{k_3} \mu_1 - \frac{k_2}{k_3} \mu_2, \quad (2.17)$$

	M_{\min}	$1.5 \times 10^{13} h^{-1} M_{\odot}$
$\sigma_{\log M}$		0.45
M_{cut}		$1.4 \times 10^{13} h^{-1} M_{\odot}$
M_1		$1.3 \times 10^{14} h^{-1} M_{\odot}$
α		1.38

Table 1. HOD parameters for the LOWZ sample [64].

with $k_3^2 = (k_2 \sin \theta_{12})^2 + (k_1 + k_2 \cos \theta_{12})^2$. Hereafter, we use the notation $\theta = \theta_{12}$. Here we followed the choice of the variables introduced in Ref. [39].

The bispectrum in the halo approach consists of the one-halo term $B_{g,1h}$, the two-halo term $B_{g,2h}$, and the three-halo term $B_{g,3h}$ given as

$$B_g(t, \mathbf{k}_1, \mathbf{k}_2, \mathbf{k}_3) = B_{g,1h}(t, \mathbf{k}_1, \mathbf{k}_2, \mathbf{k}_3) + B_{g,2h}(t, \mathbf{k}_1, \mathbf{k}_2, \mathbf{k}_3) + B_{g,3h}(t, \mathbf{k}_1, \mathbf{k}_2, \mathbf{k}_3), \quad (2.18)$$

which are written as

$$\begin{aligned} B_{g,1h}(t, \mathbf{k}_1, \mathbf{k}_2, \mathbf{k}_3) &= \frac{1}{\bar{n}^3} \int dM \frac{dn(M)}{dM} \left[\langle N_c \rangle \langle N_s(N_s - 1) \rangle (\tilde{u}(\mathbf{k}_1, M) \tilde{u}(\mathbf{k}_2, M) + 2 \text{ cyclic terms}) \right. \\ &\quad \left. + \langle N_s(N_s - 1)(N_s - 2) \rangle \tilde{u}(\mathbf{k}_1, M) \tilde{u}(\mathbf{k}_2, M) \tilde{u}(\mathbf{k}_3, M) \right], \end{aligned} \quad (2.19)$$

$$\begin{aligned} B_{g,2h}(t, \mathbf{k}_1, \mathbf{k}_2, \mathbf{k}_3) &= \frac{1}{\bar{n}^3} \int dM_1 \frac{dn(M_1)}{dM_1} \left[\langle N_c \rangle \langle N_s \rangle (\tilde{u}(\mathbf{k}_1, M_1) + \tilde{u}(\mathbf{k}_2, M_1)) \right. \\ &\quad \left. + \langle N_s(N_s - 1) \rangle \tilde{u}(\mathbf{k}_1, M_1) \tilde{u}(\mathbf{k}_2, M_1) \right] \\ &\quad \times \int dM_2 \frac{dn(M_2)}{dM_2} (\langle N_c \rangle + \langle N_c \rangle \langle N_s \rangle \tilde{u}(\mathbf{k}_3, M_2)) P_{2h}(t, \mathbf{k}_3, M_1, M_2) \\ &\quad + 2 \text{ cyclic terms}, \end{aligned} \quad (2.20)$$

$$\begin{aligned} B_{g,3h}(t, \mathbf{k}_1, \mathbf{k}_2, \mathbf{k}_3) &= \frac{1}{\bar{n}^3} \int \prod_{i=1}^3 \left[dM_i \frac{dn(M_i)}{dM_i} \langle N_c \rangle (1 + \langle N_s \rangle \tilde{u}(\mathbf{k}_i, M_i)) \right] \\ &\quad \times P_{3h}(t, \mathbf{k}_1, \mathbf{k}_2, \mathbf{k}_3, M_1, M_2, M_3), \end{aligned} \quad (2.21)$$

where N_c and N_s are the numbers of central galaxy and satellite galaxy, respectively, $\langle \dots \rangle$ denotes the averaged value per halo with fixing halo's mass under the assumption of the Poisson distribution, $\langle N_c \rangle$ and $\langle N_s \rangle$ are defined by Eqs. (2.8) and (2.9), and we use the relations $\langle N_s(N_s - 1) \rangle = \langle N_c \rangle \langle N_s \rangle^2$, $\langle N_s(N_s - 1)(N_s - 2) \rangle = \langle N_c \rangle \langle N_s \rangle^3$ (see also [40]), \bar{n} is

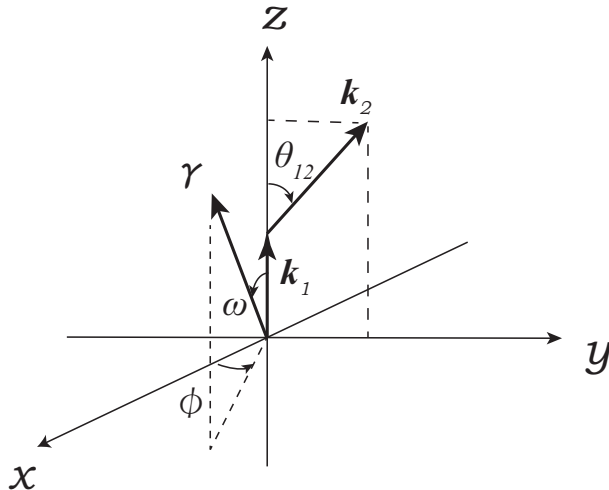


Figure 1. Definition of variables for the bispectrum.

the mean number density of galaxies given by

$$\bar{n} = \int dM \frac{dn}{dM} N_{\text{HOD}}(M), \quad (2.22)$$

and we define

$$P_{2h}(t, \mathbf{k}_3, M_1, M_2) = (b(M_1) + \mu_3^2 f)(b(M_2) + \mu_3^2 f) P_m^{\text{NL}}(t, k_3), \quad (2.23)$$

$$\begin{aligned} P_{3h}(t, \mathbf{k}_1, \mathbf{k}_2, \mathbf{k}_3, M_1, M_2, M_3) &= 2P_m^{\text{NL}}(t, k_1) P_m^{\text{NL}}(t, k_2) Z_1(\mathbf{k}_1, M_1) Z_1(\mathbf{k}_2, M_2) Z_2(\mathbf{k}_1, \mathbf{k}_2, M_3) \\ &\quad + \text{2 cyclic terms} \end{aligned} \quad (2.24)$$

with

$$Z_1(\mathbf{k}_1, M_1) = b(M_1) + f\mu_1^2, \quad (2.25)$$

$$Z_1(\mathbf{k}_2, M_2) = b(M_2) + f\mu_2^2, \quad (2.26)$$

$$\begin{aligned} Z_2(\mathbf{k}_1, \mathbf{k}_2, M_3) &= b(M_3) F_2(\mathbf{k}_1, \mathbf{k}_2) + \frac{b_2(M_3)}{2} + f\mu_{12}^2 G_2(\mathbf{k}_1, \mathbf{k}_2) \\ &\quad + \frac{1}{2} f\mu_{12} k_{12} \left\{ \frac{\mu_1}{k_1} (b(M_3) + f\mu_2^2) + \frac{\mu_2}{k_2} (b(M_3) + f\mu_1^2) \right\}, \end{aligned} \quad (2.27)$$

$\mu_{12} = (\mathbf{k}_1 + \mathbf{k}_2) \cdot \boldsymbol{\gamma} / k_{12}$, and $k_{12} = |\mathbf{k}_1 + \mathbf{k}_2|$, and where $P_m^{\text{NL}}(t, k)$ is the matter power spectrum at time t , for which we use the nonlinear fitting formula for the matter power spectrum [66]. We also use the fitting formula of the linear growth rate $f = d \log D_1(a) / d \log a = [\Omega_m(a)]^\gamma$, where $\Omega_m(a)$ is the matter density parameter at the scale factor $a = a(t)$ and $\gamma = 0.55$. For the linear bias $b(M)$, we adopt the halo bias of the fitting function,

$$b(M) = 1 - \frac{\nu^a}{\nu^a + \delta_c^a} + 0.183\nu^b + 0.265\nu^c, \quad (2.28)$$

with $a = 0.132$, $b = 1.5$, and $c = 2.4$, which was calibrated using N -body simulations [74].

3 Multipole bispectrum

3.1 Definition of multipole bispectrum

The bispectrum in redshift space is specified by 5 parameters, for which we adopt k_1 , k_2 , θ_{12} , ω , ϕ , as is described in the previous section II.B, following Ref. [39]. The parameters ω and ϕ take the values $0 \leq \omega \leq \pi$ and $0 \leq \phi \leq 2\pi$. Then, we consider the multipole expansion of the bispectrum in terms of spherical harmonics, which is usually defined as

$$Y_\ell^m(\omega, \phi) = i^{m+|m|} \sqrt{\frac{(2\ell+1)}{4\pi} \frac{(\ell-|m|)!}{(\ell+|m|)!}} P_\ell^{|m|}(\cos \omega) e^{im\phi}, \quad (3.1)$$

where m is an integer in the range $-\ell \leq m \leq \ell$, and the associated Legendre polynomials are defined by

$$P_\ell^{|m|}(\mu) = (1-\mu^2)^{|m|/2} \frac{d^{|m|}}{d\mu^{|m|}} P_\ell(\mu). \quad (3.2)$$

Note that $P_\ell^{|m=0|}(\mu)$ reduces to the Legendre polynomial $P_\ell(\mu)$.

We adopt the spherical harmonics as a set of real functions, and we define

$$Y_{\ell,m,c}(\omega, \phi) = \begin{cases} \sqrt{\frac{2\ell+1}{4\pi}} P_\ell(\cos \omega) & (m=0), \\ (-1)^{(m+|m|)/2} \sqrt{\frac{(2\ell+1)}{4\pi} \frac{(\ell-|m|)!}{(\ell+|m|)!}} P_\ell^{|m|}(\cos \omega) \sqrt{2} \cos m\phi & (m \neq 0), \end{cases} \quad (3.3)$$

$$Y_{\ell,m,s}(\omega, \phi) = (-1)^{(m+|m|)/2} \sqrt{\frac{(2\ell+1)}{4\pi} \frac{(\ell-|m|)!}{(\ell+|m|)!}} P_\ell^{|m|}(\cos \omega) \sqrt{2} \sin m\phi \quad (m \neq 0). \quad (3.4)$$

These functions satisfy the normalization

$$\int_0^{2\pi} d\phi \int_0^\pi d\omega \sin \omega Y_{\ell,m,\sigma}(\omega, \phi) Y_{\ell',m',\sigma'}(\omega, \phi) = \delta_{\ell\ell'} \delta_{mm'} \delta_{\sigma\sigma'}, \quad (3.5)$$

where σ and σ' denote c or s , though we excluded $Y_{\ell,0,s}(\omega, \phi)$ because it is zero, which is not defined.

Now we define the multipoles of the bispectrum by

$$B^{\ell,m,\sigma}(k_1, k_2, \theta) = \sqrt{\frac{1}{4\pi(2\ell+1)}} \int_0^{2\pi} d\phi \int_{-1}^{+1} d\cos \omega B_g(t, k_1, k_2, \theta, \omega, \phi) Y_{\ell,m,\sigma}(\omega, \phi). \quad (3.6)$$

The reduced bispectrum is defined in a similar way to what was done in the previous work [40]:

$$Q^{\ell,m,\sigma}(k_1, k_2, \theta) = \frac{B^{\ell,m,\sigma}(k_1, k_2, \theta)}{P^0(t, k_1)P^0(t, k_2) + P^0(t, k_2)P^0(t, k_3) + P^0(t, k_3)P^0(t, k_1)}, \quad (3.7)$$

where $P^0(t, k_i)$ is the monopole spectrum of the galaxy power spectrum $P_g(t, \mathbf{k}_i)$, i.e.,

$$P^0(t, k_i) = \frac{1}{2} \int_{-1}^{+1} d\mu P_g(t, \mathbf{k}_i). \quad (3.8)$$

In our modeling on the basis of the halo approach, $P_g(t, \mathbf{k}_i)$ is obtained by a combination of the one-halo term and the two-halo term [63]:

$$P_g(t, \mathbf{k}) = P_{g,1h}(t, \mathbf{k}) + P_{g,2h}(t, \mathbf{k}), \quad (3.9)$$

where we defined

$$P_{g,1h}(t, \mathbf{k}) = \frac{1}{\bar{n}^2} \int dM \frac{dn}{dM} \left[2 \langle N_c \rangle \langle N_s \rangle \tilde{u}(\mathbf{k}, M) + \langle N_s(N_s - 1) \rangle \tilde{u}^2(\mathbf{k}, M) \right], \quad (3.10)$$

$$P_{g,2h}(t, \mathbf{k}) = \frac{1}{\bar{n}^2} \prod_{i=1}^2 \left[\int dM_i \frac{dn}{dM_i} \langle N_c \rangle \{1 + \langle N_s \rangle \tilde{u}(\mathbf{k}, M_i)\} (b(M_i) + f\mu^2) \right] P_m^{\text{NL}}(t, k). \quad (3.11)$$

Definitions (3.6) and (3.7) reduce to those in the previous paper [40] when $m = 0$. Following the definition of the spherical harmonics (3.3) and (3.4), we list the explicit expression for the case $\ell \leq 4$ in Appendix A.

Since the bispectrum consists of a one-halo term, a two-halo term, and a three-halo term, we can express the total bispectrum as the sum of corresponding halo terms:

$$B^{\ell,m,\sigma}(k_1, k_2, \theta) = B_{1h}^{\ell,m,\sigma}(k_1, k_2, \theta) + B_{2h}^{\ell,m,\sigma}(k_1, k_2, \theta) + B_{3h}^{\ell,m,\sigma}(k_1, k_2, \theta), \quad (3.12)$$

and the reduced total bispectrum is

$$Q^{\ell,m,\sigma}(k_1, k_2, \theta) = Q_{1h}^{\ell,m,\sigma}(k_1, k_2, \theta) + Q_{2h}^{\ell,m,\sigma}(k_1, k_2, \theta) + Q_{3h}^{\ell,m,\sigma}(k_1, k_2, \theta). \quad (3.13)$$

$B^{\ell,m(\sigma)}$	$B_{1h}^{\ell,m,\sigma}$	$B_{2h}^{\ell,m,\sigma}$	$B_{3h}^{\ell,m,\sigma}$
$B^{0,0,c}$	•	•	•
$B^{2,0,c}$	•	•	•
$B^{2,1,s}$	○	○	○
$B^{2,2,c}$	○	○	○
$B^{4,0,c}$	•	•	•
$B^{4,1,s}$	○	○	○
$B^{4,2,c}$	○	○	○
$B^{4,3,s}$	○	○	○
$B^{4,4,c}$	○	○	○

Table 2. Nonvanishing multipoles of the bispectrum $B^{\ell,m,\sigma}$ up to $\ell = 4$. • means a nonvanishing quantity in previous work [40], while ○ means one found in this work.

3.2 Results

We demonstrate the characteristic behaviors of the multipole bispectrum defined in the previous subsection. There are nine nonvanishing components of $B^{\ell,m,\sigma}$ up to $\ell = 4$ (see Table 2), of which 3 multipoles with $m = 0$ have been known so far [39, 41]; these we investigated in our previous work [40], while six multipoles denoted by the symbol ○ in the table are the new components, which we investigated in the present paper. The other components up to $\ell = 4$ are zero, because of the symmetry with respect to ϕ .

Figure 2 shows the characteristic behaviors of the new nonzero components, where we adopted the HOD parameters of the LOWZ sample in Table I. Each panel of Fig. 2 plots $Q^{2,1,s}$, $Q^{2,2,c}$, $Q^{4,1,s}$, $Q^{4,2,c}$, $Q^{4,3,s}$, and $Q^{4,4,c}$ as functions of θ with k_1 and $k_2 = 2k_1$ fixed. Each multipole bispectrum shows unique behaviors. One can see that the one-halo term (green dotted curve) and the two-halo term (blue dashed curve) make significant contributions to these multipole bispectrum and dominate over the contribution from the three-halo term (red long-dashed curve) for the case $k_1 > 0.1 \text{ Mpc}^{-1}$. This is significant for $Q^{4,1,s}$, $Q^{4,2,c}$, $Q^{4,3,s}$, and $Q^{4,4,c}$ than $Q^{2,1,s}$ and $Q^{2,2,c}$.

The contributions of the two-halo term and the one-halo term are opposite compared with the three-halo term for $Q^{2,1,s}$ and $Q^{2,2,c}$. This is also true for $Q^{2,0,c}$ investigated in the previous work [40]. This can be understood as follows: The higher multipole bispectrum reflects the redshift space distortions. The contributions of the two-halo term and the one-halo term reflect the FoG effect, while the three-halo term contribution reflect the linear distortion. These two redshift-space distortions have an opposite effect in the quadrupole power spectrum and bispectrum.

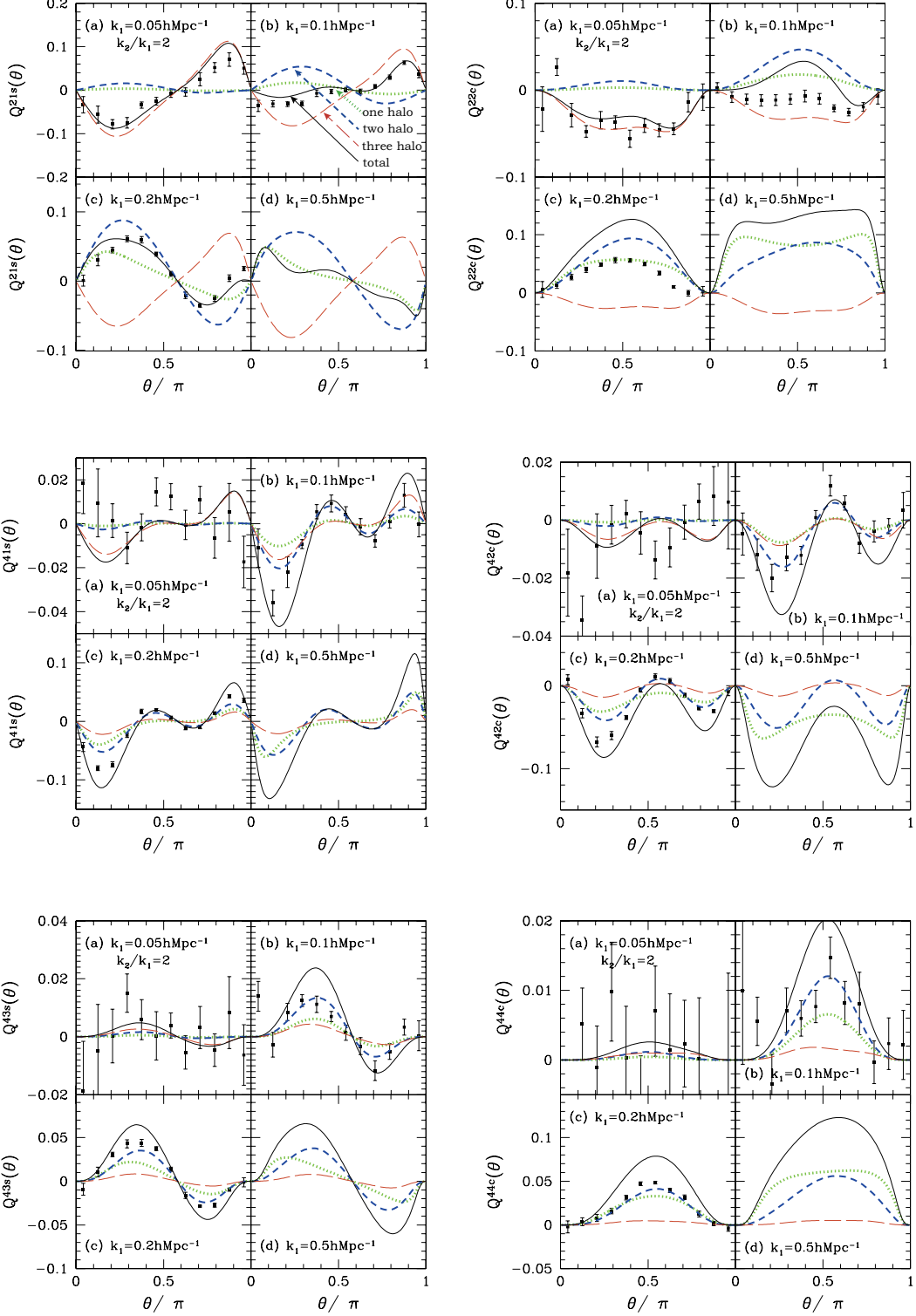


Figure 2. Nonvanishing multipoles of the reduced bispectrum, $Q^{2,1,s}$, $Q^{2,2,c}$, $Q^{4,1,s}$, $Q^{4,2,c}$, $Q^{4,3,s}$, and $Q^{4,4,c}$ as function of θ for the LOWZ sample by fixing (a) $k_1 = 0.05$, (b) $k_1 = 0.1$, (c) $k_1 = 0.2$, and (d) $k_1 = 0.5$ in units of h/Mpc and $k_2/k_1 = 2$. In each panel the (green) dotted curve is the one-halo term contribution, the (blue) short-dashed curve is the two-halo term contribution, the (red) long-dashed curve is the three-halo term contribution, and the (black) solid curve is the total combination. Here we set $b_2 = 0$. The data points with error bars show the results of the mock catalogs. Result of the mock catalog for the case $k_1 = 0.5$ is not available due to lack of the resolution of our simulation.

3.3 Comparison with the results of mock catalogs

We compare our analytic model with the results of mock catalogs by assuming the HOD of the SDSS-III BOSS LOWZ sample. A similar comparison was done for $Q^{0,0}$, $Q^{2,0}$, and $Q^{4,0}$ in our previous paper [40], which is also adopted for comparison in the present paper. We run 10 realizations of N -body simulations at a side length of $1h^{-1}$ Gpc with the number of mass particles set as 800^3 (where the mass for each particle is set as $1.3 \times 10^{11} h^{-1} M_\odot$) using the Gadget-2 code [75]. The softening length is set to be $50h^{-1}$ kpc. The initial mass distribution is Gaussian, starting from $z = 49$ generated by the 2LPT code of [76]. The halo is identified with the friends-of-friends algorithm with a linking length of 0.2. The minimum number of mass particles is 10, corresponding to a mass of $1.3 \times 10^{12} h^{-1} M_\odot$. The central and satellite galaxies are assigned to each halo to follow the HOD of the BOSS LOWZ sample. The position and velocity of each central galaxy are given as the arithmetic mean of all particles in the halo. The position and velocity of satellites are defined as those of randomly selected mass particles. We confirmed that the mass resolution of our simulation is sufficient for the following comparison with our theoretical model.

The data points with error bars in Fig. 2 show the result of the mock catalogs. The error bars represent the one-sigma dispersion of 10 simulation results divided by $\sqrt{10}$, which roughly corresponds to the sample variance for $10 (\text{Gpc}/h)^3$ volume data. As is demonstrated in [40] for $Q^{0,0,c}$, $Q^{2,0,c}$, and $Q^{4,0,c}$, our theoretical model well explains the characteristic behavior of the bispectrum from the mock catalogs even for $Q^{\ell,m,\sigma}$ with $m \neq 0$, though some differences arise for the cases with larger wavenumbers at a quantitative level. However, the behaviors of the simulations are reproduced at a qualitative level. Behaviors of the galaxy bispectrum at large wavenumbers have not been well studied. One of the reason might be the galaxy bispectrum sensitively depends on the HOD parameter as our result suggests. Even for the halo bispectrum, we don't know a precise formula which reproduces the three halo term being valid at higher wavenumbers. Our analytic model of the three halo term is the simplest model based on the lowest order of density perturbations, which must be improved for comparison with mock catalogs or observations in future.

4 Discussion: approximate formulas

In this section, we consider approximate formulas, which roughly explain the characteristic behaviors of the multipoles of the bispectrum. Since these formulas are too long to be fully presented in the main part, they are listed in Appendix B. These approximate formulas are useful for understanding the behaviors of the multipole bispectrum.

According to previous works [40, 63], we may introduce the following approximate formulas for the one-halo term, the two-halo term, and the three-halo term:

$$B_{g,1h}(t, \mathbf{k}_1, \mathbf{k}_2, \mathbf{k}_3) \simeq \frac{f_s^2}{\bar{n}^2} (\tilde{u}(\mathbf{k}_1)\tilde{u}(\mathbf{k}_2) + \tilde{u}(\mathbf{k}_2)\tilde{u}(\mathbf{k}_3) + \tilde{u}(\mathbf{k}_3)\tilde{u}(\mathbf{k}_1)), \quad (4.1)$$

$$B_{g,2h}(t, \mathbf{k}_1, \mathbf{k}_2, \mathbf{k}_3) \simeq \frac{f_s}{\bar{n}} (\tilde{u}(\mathbf{k}_1) + \tilde{u}(\mathbf{k}_2)) (\bar{b} + \mu_3^2 f)^2 P_m^{\text{NL}}(k_3) + 2 \text{ cyclic terms}, \quad (4.2)$$

$$\begin{aligned} B_{g,3h}(t, \mathbf{k}_1, \mathbf{k}_2, \mathbf{k}_3) \simeq & 2P_m^{\text{NL}}(t, k_1)P_m^{\text{NL}}(t, k_2)(\bar{b} + \mu_1^2 f)(\bar{b} + \mu_2^2 f) [\bar{b}F_2(\mathbf{k}_1, \mathbf{k}_2) + f\mu_3^2 G_2(\mathbf{k}_1, \mathbf{k}_2) + \frac{\bar{b}_2}{2} \\ & - \frac{1}{2}f\mu_3 k_3 \left(\frac{\mu_1}{k_1}(\bar{b} + f\mu_2^2) + \frac{\mu_2}{k_2}(\bar{b} + f\mu_1^2) \right)] + 2 \text{ cyclic terms}, \end{aligned} \quad (4.3)$$

respectively, where we use the approximate formula

$$\tilde{u}(\mathbf{k}_i) \simeq \exp \left[-\frac{\bar{\sigma}_{v,\text{off}}^2 k_i^2 \mu^2}{2a^2 H^2(z)} \right] = \exp \left[-\lambda^2 k_i^2 \mu^2 \right], \quad (4.4)$$

for $i = 1, 2$, and 3 , where \bar{b} and $\bar{\sigma}_{v,\text{off}}$ are averaged values of the bias and the random velocity of satellite galaxies over the halo mass and f_s is the satellite fraction. Here we introduce the characteristic length scale, associated with the random motions by

$$\lambda^2 = \frac{\bar{\sigma}_{v,\text{off}}^2}{2a^2 H^2(z)}, \quad (4.5)$$

where $aH(z)$ is the value at the mean redshift \bar{z} as $aH(z) = H(\bar{z})/(1 + \bar{z})$.

Then, we may write the approximate formula for the multipole bispectrum in the form expressing the dependence on f_s/\bar{n} explicitly as

$$B^{\ell,m,\sigma}(k_1, k_2, \theta) = \frac{f_s^2}{\bar{n}^2} \tilde{B}_{1h}^{\ell,m,\sigma}(k_1, k_2, \theta) + \frac{f_s}{\bar{n}} \tilde{B}_{2h}^{\ell,m,\sigma}(k_1, k_2, \theta) + \tilde{B}_{3h}^{\ell,m,\sigma}(k_1, k_2, \theta), \quad (4.6)$$

where the formulas of $\tilde{B}^{\ell,m,\sigma}$ are presented in Appendix B.

The mathematical formulas of Appendix B are derived using *Mathematica*. The source *Mathematica* programs for the derivation are provided in the source file of arXiv:1706.03515.

From the approximation formulas, in general, we have

$$B_{1h}^{\ell,m,\sigma} \sim \left(\frac{f_s}{\bar{n}} \right)^2 (\lambda k)^\ell \sin^m \theta_{12}, \quad (4.7)$$

$$B_{2h}^{\ell,m,\sigma} \sim \frac{f_s}{\bar{n}} \left[\left(\mathcal{O}(b^2 P_m) + \mathcal{O}(bf P_m) + \mathcal{O}(f^2 P_m) \right) + \mathcal{O}(\lambda^2 k^2 P_g) \right] \sin^m \theta_{12}, \quad (4.8)$$

$$B_{3h}^{\ell,m,\sigma} \sim f^{\ell/2} \mathcal{O}(P_m^2) \sin^m \theta_{12}. \quad (4.9)$$

The factor $\sin^m \theta_{12}$ comes from the mathematical properties of spherical harmonics.

For the case $\ell = 0$, as discussed in Ref. [40], $B_{1h}^{0,0,c}(k_1, k_2, \theta) \simeq \frac{f_s^2}{\bar{n}^2} (3 - \mathcal{O}(k^2 \lambda^2))$. Thus, Eq. (4.7) means that the one-halo term makes a contribution to the multipole bispectrum dominantly from the term in proportion to $(k\lambda)^\ell$, which comes from the FoG effect. Equation (4.9) reveals that the three-halo term is in proportion to the factor $f^{\ell/2}$, where f denotes the linear growth rate, which shows that the three-halo term contribution comes from the linear redshift-space distortion. The contribution from the two-halo term includes both the FoG effect and the linear redshift-space distortion effect depending on the scales k , from Eq. (4.8). In the two-halo term, the FoG effect is the dominant contribution for scales larger than $k \sim 0.1 \text{ Mpc}^{-1}$. The total combination of the one-halo term, the two-halo term, and the three-halo term contributes to the complicated behaviors of the multipole bispectrum.

5 Summary and Conclusions

In this work, as a generalization of the halo approach to the galaxy bispectrum in redshift space, we found six new nonvanishing multipole components up to $\ell = 4$. We demonstrated the characteristic behaviors of these nonvanishing multipoles, assuming the HOD parameters of the LOWZ sample. Each component shows unique behaviors. Using an analytic approximate method, we investigated how the one-halo term, the two-halo term, and the three-halo

term make contributions to the multipole bispectrum. This has revealed that the higher multipole bispectrum is significantly contaminated by the FoG effect on scales larger than $k \sim 0.1 \text{ Mpc}^{-1}$. The total bispectrum is determined by the balance between the contributions of the FoG effect and the linear redshift-space distortion and is complicated. This study shows that the bispectrum reflects the cosmological model and the physical properties of the galaxy sample. These properties are interesting because we might be able to test the cosmological model as well as the galaxy–halo connection, leading to better understandings of the large-scale structure formation.

A more precise theoretical model will be necessary to extract cosmological information from observational data of ongoing and future galaxy redshift surveys (e.g., SDSS IV, Subaru/PFS, and EUCLID), which will be a necessary investigation as an extension to our model. Because the validity of standard perturbation theory at leading order is somehow limited to the linear regime, this limits the validity of $P_{2h}(t, k_1, k_2, M_1, M_2)$ and $P_{3h}(t, k_1, k_2, k_3, M_1, M_2, M_3)$. More precise evaluation of the nonlinearity including the next-to-leading order correction and higher order corrections is needed for further extension. As an example, in Ref. [33], a model for the matter bispectrum considering one-loop order correction in redshift space has been developed by introducing a univariate function with a single free parameter. Improvement of modeling the correlation of halos by including the higher order corrections will be necessary in the future.

Acknowledgment

This work was supported by MEXT/JSPS KAKENHI Grant Numbers 15H05895 and JP16H03977. We thank A. Taruya, I. Hashimoto, Y. Rasera, T. Nishimichi, N. Yoshida, M. Takada, and N. Sugiyama for useful comments.

A Spherical Harmonics

$$\begin{aligned}
Y_{0,0} &= \frac{1}{\sqrt{4\pi}}, \quad Y_{1,0} = \sqrt{\frac{3}{4\pi}} \cos \omega, \quad Y_{1,1,c} = -\sqrt{\frac{3}{4\pi}} \sin \omega \cos \phi, \quad Y_{11s} = -\sqrt{\frac{3}{4\pi}} \sin \omega \sin \phi, \\
Y_{2,0} &= \sqrt{\frac{5}{16\pi}} (3 \cos^2 \omega - 1), \quad Y_{2,1,c} = -\sqrt{\frac{15}{4\pi}} \sin \omega \cos \omega \cos \phi, \quad Y_{2,1,s} = -\sqrt{\frac{15}{4\pi}} \sin \omega \cos \omega \sin \phi, \\
Y_{2,2,c} &= +\sqrt{\frac{15}{16\pi}} \sin^2 \omega \cos 2\phi, \quad Y_{2,2,s} = +\sqrt{\frac{15}{16\pi}} \sin^2 \omega \sin 2\phi, \quad Y_{3,0} = \sqrt{\frac{7}{16\pi}} (5 \cos^3 \omega - 3 \cos \omega), \\
Y_{3,1,c} &= -\sqrt{\frac{21}{32\pi}} \sin \omega (5 \cos^2 \omega - 1) \cos \phi, \quad Y_{3,1,s} = -\sqrt{\frac{21}{32\pi}} \sin \omega (5 \cos^2 \omega - 1) \sin \phi, \\
Y_{3,2,c} &= +\sqrt{\frac{105}{16\pi}} \sin^2 \omega \cos \omega \cos 2\phi, \quad Y_{3,2,s} = +\sqrt{\frac{105}{16\pi}} \sin^2 \omega \cos \omega \sin 2\phi, \\
Y_{3,3,c} &= -\sqrt{\frac{35}{32\pi}} \sin^3 \omega \cos 3\phi, \quad Y_{3,3,s} = -\sqrt{\frac{35}{32\pi}} \sin^3 \omega \sin 3\phi, \\
Y_{4,0} &= \sqrt{\frac{9}{256\pi}} (35 \cos^4 \omega - 30 \cos^2 \omega + 3), \\
Y_{4,1,c} &= -\sqrt{\frac{45}{32\pi}} \sin \omega (7 \cos^2 \omega - 3) \cos \omega \cos \phi, \quad Y_{4,1,s} = -\sqrt{\frac{45}{32\pi}} \sin \omega (7 \cos^2 \omega - 3) \cos \omega \sin \phi, \\
Y_{4,2,c} &= +\sqrt{\frac{45}{64\pi}} (-7 \cos^4 \omega + 8 \cos^2 \omega - 1) \cos 2\phi, \quad Y_{4,2,s} = +\sqrt{\frac{45}{64\pi}} (-7 \cos^4 \omega + 8 \cos^2 \omega - 1) \sin 2\phi, \\
Y_{4,3,c} &= -\sqrt{\frac{315}{32\pi}} \sin^3 \omega \cos \omega \cos 3\phi, \quad Y_{4,3,s} = -\sqrt{\frac{315}{32\pi}} \sin^3 \omega \cos \omega \sin 3\phi, \\
Y_{4,4,c} &= +\sqrt{\frac{315}{256\pi}} \sin^4 \omega \cos 4\phi, \quad Y_{4,4,s} = +\sqrt{\frac{315}{256\pi}} \sin^4 \omega \sin 4\phi,
\end{aligned}$$

B Approximate formulas

$$\begin{aligned}
\tilde{B}_{1h}^{2,1,s} &= \frac{1}{1155\sqrt{3}} \lambda^2 k_2 \sin \theta_{12} (k_1 + 2k_2 \cos \theta_{12}) \left\{ 924 - 594\lambda^2 \left(k_1^2 + k_1 k_2 \cos \theta_{12} + k_2^2 \right) \right. \\
&\quad + 33\lambda^4 \left[5k_1^4 + k_1 k_2 (5 \cos \theta_{12} (k_1^2 + 2k_2^2) + 3k_1 k_2 \cos 2\theta_{12}) + 7k_1^2 k_2^2 + 5k_2^4 \right] \\
&\quad - 5\lambda^6 \left[7k_1^6 + 5k_1^4 k_2^2 + 12k_1^2 k_2^4 + k_1 k_2 (k_1 k_2 (\cos 2\theta_{12} (2k_1^2 + 9k_2^2) + k_1 k_2 \cos 3\theta_{12}) + \right. \\
&\quad \left. \left. \cos \theta_{12} (7k_1^4 + 6k_1^2 k_2^2 + 21k_2^4)) + 7k_2^6 \right] \right\} \tag{B.1}
\end{aligned}$$

$$\begin{aligned}
\tilde{B}_{1h}^{2,2,c} = & \frac{1}{2310\sqrt{3}}\lambda^2 k_2^2 \sin^2 \theta_{12} \left\{ 1848 - 594\lambda^2 \left(k_1^2 + 2k_1 k_2 \cos \theta_{12} + 2k_2^2 \right) \right. \\
& + 33\lambda^4 \left[3k_1^4 + 2k_1 k_2 (2 \cos \theta_{12} (2k_1^2 + 5k_2^2) + 3k_1 k_2 \cos 2\theta_{12}) + 12k_1^2 k_2^2 + 10k_2^4 \right] \\
& - \lambda^6 \left[15k_1^6 + 27k_1^4 k_2^2 + 135k_1^2 k_2^4 + 2k_1 k_2 \left(k_1 k_2 (9 \cos 2\theta_{12} (k_1^2 + 5k_2^2) + 5k_1 k_2 \cos 3\theta_{12}) \right. \right. \\
& \left. \left. + 15 \cos \theta_{12} (k_1^4 + 3k_1^2 k_2^2 + 7k_2^4)) + 70k_2^6 \right] \right\} \tag{B.2}
\end{aligned}$$

$$\begin{aligned}
\tilde{B}_{1h}^{4,1,s} = & \frac{1}{12012\sqrt{10}}\lambda^4 k_2 \sin \theta_{12} (k_1 + 2k_2 \cos \theta_{12}) \left\{ -572 \left(8k_1^2 + 8k_1 k_2 \cos \theta_{12} + 7k_2^2 \cos 2\theta_{12} + k_2^2 \right) \right. \\
& + 26\lambda^2 \left[80k_1^4 + 5k_1 k_2 \cos \theta_{12} (16k_1^2 + 25k_2^2) + 84k_1^2 k_2^2 + \cos 2\theta_{12} (76k_1^2 k_2^2 + 70k_2^4) + 35k_1 k_2^3 \cos 3\theta_{12} + 10k_2^4 \right] \\
& - 5\lambda^4 \left[112k_1^6 + 66k_1^4 k_2^2 + 143k_1^2 k_2^4 + k_1 k_2^3 (\cos 3\theta_{12} (23k_1^2 + 98k_2^2) + 21k_1 k_2 \cos 4\theta_{12}) \right. \\
& \left. \left. + k_1 k_2 \cos \theta_{12} (112k_1^4 + 89k_1^2 k_2^2 + 238k_2^4) + 2k_2^2 \cos 2\theta_{12} (23k_1^4 + 86k_1^2 k_2^2 + 49k_2^4) + 14k_2^6 \right] \right\} \tag{B.3}
\end{aligned}$$

$$\begin{aligned}
\tilde{B}_{1h}^{4,2,c} = & \frac{1}{12012\sqrt{5}}\lambda^4 k_2^2 \sin^2 \theta_{12} \left\{ -572 \left(6k_1^2 + 12k_1 k_2 \cos \theta_{12} + 7k_2^2 \cos 2\theta_{12} + 5k_2^2 \right) \right. \\
& + 26\lambda^2 \left[36k_1^4 + k_1 k_2 \cos \theta_{12} (96k_1^2 + 205k_2^2) + k_2^2 \cos 2\theta_{12} (93k_1^2 + 70k_2^2) + 123k_1^2 k_2^2 + 35k_1 k_2^3 \cos 3\theta_{12} + 50k_2^4 \right] \\
& - \lambda^4 \left[180k_1^6 + 303k_1^4 k_2^2 + 1305k_1^2 k_2^4 + 5k_1 k_2^3 (\cos 3\theta_{12} (38k_1^2 + 98k_2^2) + 21k_1 k_2 \cos 4\theta_{12}) \right. \\
& \left. \left. + 10k_1 k_2 \cos \theta_{12} (36k_1^4 + 101k_1^2 k_2^2 + 203k_2^4) + k_2^2 \cos 2\theta_{12} (237k_1^4 + 1290k_1^2 k_2^2 + 490k_2^4) + 350k_2^6 \right] \right\} \tag{B.4}
\end{aligned}$$

$$\begin{aligned}
\tilde{B}_{1h}^{4,3,s} = & \frac{1}{429\sqrt{70}}\lambda^4 k_2^3 \sin^3 \theta_{12} (k_1 + 2k_2 \cos \theta_{12}) \left\{ 286 - 26\lambda^2 \left(2k_1^2 + 5k_1 k_2 \cos \theta_{12} + 5k_2^2 \right) \right. \\
& + 5\lambda^4 \left[k_1^4 + k_1^3 k_2 \cos \theta_{12} + k_1^2 k_2^2 (3 \cos 2\theta_{12} + 5) + 14k_1 k_2^3 \cos \theta_{12} + 7k_2^4 \right] \left. \right\} \tag{B.5}
\end{aligned}$$

$$\begin{aligned}
\tilde{B}_{1h}^{4,4,c} = & \frac{1}{1716\sqrt{35}}\lambda^4 k_2^4 \sin^4 \theta_{12} \left\{ 572 - 26\lambda^2 \left(3k_1^2 + 10k_1 k_2 \cos \theta_{12} + 10k_2^2 \right) \right. \\
& + \lambda^4 \left[3k_1^4 + 20k_1^3 k_2 \cos \theta_{12} + 30k_1^2 k_2^2 (\cos 2\theta_{12} + 2) + 140k_1 k_2^3 \cos \theta_{12} + 70k_2^4 \right] \left. \right\} \tag{B.6}
\end{aligned}$$

$$\begin{aligned}
\tilde{B}_{2h}^{2,1,s} = & \frac{1}{1155\sqrt{3}(k_1^2 + 2\cos\theta_{12}k_2k_1 + k_2^2)^2} \\
& \left\{ 2P_m(k_1) \sin\theta_{12}(k_1 + 2\cos\theta_{12}k_2)k_2(k_1^2 + 2\cos\theta_{12}k_2k_1 + k_2^2)^2 \lambda^2 \left[11(21b^2 + 18fb + 5f^2) \right. \right. \\
& - \lambda^2 \left[(99b^2 + 110fb + 35f^2)k_1^2 + (99b^2 + 110fb + 35f^2)\cos\theta_{12}k_2k_1 + (99b^2 + 88fb + 25f^2)k_2^2 \right. \\
& \left. \left. + 2f(11b + 5f)\cos 2\theta_{12}k_2^2 \right] \right] \\
& - P_m(k_2)(k_1^2 + 2\cos\theta_{12}k_2k_1 + k_2^2)^2 \left[132f(7b + 3f)\sin 2\theta_{12} - 11\lambda^2 \left[2f(f\sin 4\theta_{12}k_1 + (9b + 5f)\sin 3\theta_{12}k_2)k_1 \right. \right. \\
& + 2(21b^2 + 27fb + 10f^2)\sin\theta_{12}k_2k_1 + \sin 2\theta_{12}(4f(9b + 4f)k_1^2 + 3(b + f)(7b + 5f)k_2^2) \left. \right] \\
& + 2\sin\theta_{12}\lambda^4 \left[k_1 \left(2(99b^2 + 165fb + 70f^2)k_2^3 + 9(11b^2 + 22fb + 10f^2)k_1^2k_2 + \cos 2\theta_{12}(4f(33b + 20f)k_1^2 \right. \right. \\
& \left. \left. + (99b^2 + 220fb + 105f^2)k_2^2)k_2 + k_1f \left(5f\cos 4\theta_{12}k_1k_2 + \cos 3\theta_{12}(66bk_2^2 + 5f(2k_1^2 + 9k_2^2)) \right) \right) \right. \\
& \left. + \cos\theta_{12} \left(10f(11b + 6f)k_1^4 + 27(11b^2 + 22fb + 10f^2)k_2^2k_1^2 + (99b^2 + 165fb + 70f^2)k_2^4 \right) \right] \\
& - P_m(k_3)k_2 \left[264f(7b + 3f)(k_1 + \cos\theta_{12}k_2)(k_1^2 + 2\cos\theta_{12}k_2k_1 + k_2^2)\sin\theta_{12} \right. \\
& - 11\lambda^2 \left[k_2 \left(k_1k_2 \left((21b^2 + 18fb + 7f^2)\sin 4\theta_{12}k_1k_2 + \sin 3\theta_{12}(42(k_1^2 + k_2^2)b^2 + 54f(k_1^2 + k_2^2)b + 4f^2(6k_1^2 + 5k_2^2)) \right) \right. \right. \\
& + \sin 2\theta_{12} \left((21b^2 + 72fb + 35f^2)k_1^4 + 4(21b^2 + 36fb + 14f^2)k_2^2k_1^2 + 3(b + f)(7b + 5f)k_2^4 \right) \left. \right] \\
& + 2\sin\theta_{12}k_1 \left(2f(9b + 5f)k_1^4 + 3(7b^2 + 21fb + 8f^2)k_2^2k_1^2 + (21b^2 + 45fb + 20f^2)k_2^4 \right) \left. \right] \\
& + \lambda^4 \left[k_1 \sin\theta_{12} \left(10f(11b + 7f)k_1^6 + 15f(11b + 5f)k_2^2k_1^4 + 2(99b^2 + 154fb + 50f^2)k_2^4k_1^2 \right. \right. \\
& + (198b^2 + 385fb + 175f^2)k_2^6 \left. \right) + k_2 \left(k_1k_2 \left(f(11b + 5f)k_1 \sin 5\theta_{12}k_2 + \sin 4\theta_{12}(f(11b + 10f)k_1^2 \right. \right. \\
& + (99b^2 + 121fb + 45f^2)k_2^2) \left. \right) + \sin 3\theta_{12} \left(5f(11b + 9f)k_1^4 + (198b^2 + 209fb + 75f^2)k_2^2k_1^2 \right. \\
& \left. \left. + (198b^2 + 275fb + 105f^2)k_2^4 \right) \right) + \sin 2\theta_{12} \left(15f(11b + 7f)k_1^6 + (99b^2 + 143fb + 50f^2)k_2^2k_1^4 \right. \\
& \left. \left. + (396b^2 + 583fb + 225f^2)k_2^4k_1^2 + (99b^2 + 165fb + 70f^2)k_2^6 \right) \right) \right] \Bigg\} \quad (B.7)
\end{aligned}$$

$$\begin{aligned}
\tilde{B}_{2h}^{2,2,c} = & \frac{\sin^2 \theta_{12}}{1155\sqrt{3}(k_1^2 + 2\cos\theta_{12}k_2k_1 + k_2^2)^2} \\
& \left\{ P_m(k_1)k_2^2(k_1^2 + 2\cos\theta_{12}k_2k_1 + k_2^2)^2 \lambda^2 \left[22(21b^2 + 6fb + f^2) - \lambda^2 \left[3(33b^2 + 22fb + 5f^2)k_1^2 \right. \right. \right. \\
& + 6(33b^2 + 22fb + 5f^2)\cos\theta_{12}k_2k_1 + 2(99b^2 + 44fb + 9f^2)k_2^2 + 4f(11b + 3f)\cos 2\theta_{12}k_2^2 \left. \left. \right] \right] \\
& - P_m(k_2)(k_1^2 + 2\cos\theta_{12}k_2k_1 + k_2^2)^2 \left[132f(7b + 3f) - 11\lambda^2 \left[4f(3b + 2f)k_1^2 \right. \right. \\
& + 4f \left(f\cos 2\theta_{12}k_1 + (9b + 5f)\cos\theta_{12}k_2 \right) k_1 + 3(b + f)(7b + 5f)k_2^2 \left. \right] + \lambda^4 \left[2f(11b + 9f)k_1^4 \right. \\
& + 3(33b^2 + 88fb + 45f^2)k_2^2k_1^2 + 2 \left(f \left(5f\cos 3\theta_{12}k_1k_2 + \cos 2\theta_{12}(6fk_1^2 + 66bk_2^2 + 45fk_2^2) \right) k_1 \right. \\
& + \cos\theta_{12}k_2 \left(3f(22b + 15f)k_1^2 + (99b^2 + 220fb + 105f^2)k_2^2 \right) \left. \right) k_1 + (99b^2 + 165fb + 70f^2)k_2^4 \left. \right] \\
& - P_m(k_3)k_2^2 \left[132f(7b + 3f)(k_1^2 + 2\cos\theta_{12}k_2k_1 + k_2^2) - 11\lambda^2 \left[(21b^2 + 12fb + 7f^2)k_1^4 \right. \right. \\
& + 28(3b^2 + 3fb + f^2)k_2^2k_1^2 + 2 \left((21b^2 + 18fb + 7f^2)\cos 2\theta_{12}k_1k_2 + 2\cos\theta_{12} \left(3(7b^2 + 5fb + 2f^2)k_1^2 \right. \right. \\
& + (21b^2 + 27fb + 10f^2)k_2^2 \left. \right) \left. \right) k_2k_1 + 3(b + f)(7b + 5f)k_2^4 \left. \right] + \lambda^4 \left[f(11b + 15f)k_1^6 \right. \\
& + (99b^2 + 55fb + 18f^2)k_2^2k_1^4 + 3(132b^2 + 143fb + 45f^2)k_2^4k_1^2 + 2 \left(\left(f(11b + 5f)\cos 3\theta_{12}k_1k_2 \right. \right. \\
& + \cos 2\theta_{12} \left(f(11b + 6f)k_1^2 + (99b^2 + 121fb + 45f^2)k_2^2 \right) \left. \right) k_1k_2 + \cos\theta_{12} \left(15(k_1^4 + 3k_2^2k_1^2 + 7k_2^4)f^2 \right. \\
& + 11b(k_1^4 + 15k_2^2k_1^2 + 25k_2^4)f + 198b^2k_2^2(k_1^2 + k_2^2) \left. \right) \left. \right) k_2k_1 + (99b^2 + 165fb + 70f^2)k_2^6 \left. \right] \left. \right\} \quad (B.8)
\end{aligned}$$

$$\begin{aligned}
\tilde{B}_{2h}^{4,1,s} = & \frac{1}{36036\sqrt{10}(k_1^2 + 2\cos\theta_{12}k_2k_1 + k_2^2)^2} \\
& \left\{ 4P_m(k_1)\lambda^2k_2(k_1^2 + 2\cos\theta_{12}k_2k_1 + k_2^2)^2(k_1 + 2\cos\theta_{12}k_2)\sin\theta_{12} \left[208f(11b + 5f) - \lambda^2 \left[8(143b^2 + 260fb + 105f^2)k_1^2 \right. \right. \right. \\
& + 8(143b^2 + 260fb + 105f^2)\cos\theta_{12}k_2k_1 + (143b^2 + 1118fb + 495f^2)k_2^2 + (1001b^2 + 962fb + 345f^2)\cos 2\theta_{12}k_2^2 \left. \left. \left. \right] \right] \\
& - P_m(k_2)(k_1^2 + 2\cos\theta_{12}k_2k_1 + k_2^2)^2 \left[572f^2(2\sin 2\theta_{12} + 7\sin 4\theta_{12}) \right. \\
& - 26\lambda^2f \left[2(33b + 20f)\sin\theta_{12}k_1k_2 + 15(22b + 13f)\sin 3\theta_{12}k_1k_2 + 35f\sin 5\theta_{12}k_1k_2 \right. \\
& + 2\sin 2\theta_{12} \left(2(88b + 43f)k_1^2 + (22b + 15f)k_2^2 \right) + \sin 4\theta_{12}(74fk_1^2 + 7(22b + 15f)k_2^2) \left. \right] \\
& + \lambda^4 \left[315f^2\sin 6\theta_{12}k_1^2k_2^2 + 10f\sin 5\theta_{12}k_1k_2(66fk_1^2 + 7(26b + 21f)k_2^2) \right. \\
& + 6\sin 3\theta_{12}k_1 \left(6f(169b + 100f)k_1^2 + 5(143b^2 + 338fb + 168f^2)k_2^2 \right)k_2 + 2\sin\theta_{12}k_1k_2 \left(2(1144b^2 \right. \\
& \left. + 1677fb + 675f^2)k_1^2 + (429b^2 + 1040fb + 525f^2)k_2^2 \right) + \sin 2\theta_{12} \left(20f(208b + 99f)k_1^4 \right. \\
& \left. + 3(2288b^2 + 4472fb + 2025f^2)k_2^2k_1^2 + 2(143b^2 + 390fb + 210f^2)k_2^4 \right) \\
& + \sin 4\theta_{12} \left(690f^2k_1^4 + 6f(962b + 675f)k_2^2k_1^2 + 7(143b^2 + 390fb + 210f^2)k_2^4 \right) \left. \right] \\
& - P_m(k_3)k_2 \left[1144f^2 \left(16k_1^3 + 30\cos 2\theta_{12}k_2^2k_1 + 18k_2^2k_1 + 7\cos 3\theta_{12}k_2^3 + \cos\theta_{12}(9k_2^3 + 48k_1^2k_2) \right) \sin\theta_{12} \right. \\
& - 26\lambda^2f \left[\left((14(11b + 5f)\sin 5\theta_{12}k_1k_2^2 + \sin 4\theta_{12}k_2((484b + 259f)k_1^2 + 7(22b + 15f)k_2^2) \right. \right. \\
& + 2\sin 3\theta_{12}k_1((341b + 234f)k_1^2 + 3(88b + 65f)k_2^2) \left. \right)k_2 + 2\sin 2\theta_{12} \left(8(44b + 35f)k_1^4 + (396b + 301f)k_1^2k_2^2 \right. \\
& \left. \left. +(22b + 15f)k_2^4 \right) \right)k_2 + 2\sin\theta_{12}k_1(16(11b + 10f)k_1^4 + (385b + 258f)k_2^2k_1^2 + 5(11b + 8f)k_2^4) \right] \\
& + \lambda^4 \left[2k_1 \left(80f(26b + 21f)k_1^6 + 15f(208b + 99f)k_2^2k_1^4 + 2(143b^2 + 819fb + 675f^2)k_2^4k_1^2 \right. \right. \\
& \left. \left. +(286b^2 + 910fb + 525f^2)k_2^6 \right) \sin\theta_{12} - k_2 \left(k_2 \left(k_1k_2 \left(-7(143b^2 + 130fb + 45f^2)k_1 \sin 6\theta_{12}k_2 \right. \right. \right. \right. \\
& \left. \left. \left. \left. - 2\sin 5\theta_{12}(1001(k_1^2 + k_2^2)b^2 + 52f(18k_1^2 + 35k_2^2)b + 15f^2(22k_1^2 + 49k_2^2)) \right) - ((1001b^2 + 962fb + 690f^2)k_1^4 \right. \right. \\
& \left. \left. + 6(715b^2 + 1612fb + 675f^2)k_2^2k_1^2 + 7(143b^2 + 390fb + 210f^2)k_2^4) \sin 4\theta_{12} \right) - 2k_1 \sin 3\theta_{12}(5f(208b + 237f)k_1^4 \right. \\
& \left. + 3(429b^2 + 1378fb + 600f^2)k_2^2k_1^2 + 3(429b^2 + 1430fb + 840f^2)k_2^4) \right) - \sin 2\theta_{12} \left(240f(26b + 21f)k_1^6 \right. \\
& \left. + 2(143b^2 + 2158fb + 990f^2)k_2^2k_1^4 + 3(715b^2 + 3042fb + 2025f^2)k_2^4k_1^2 \right. \\
& \left. + 2(143b^2 + 390fb + 210f^2)k_2^6 \right) \left. \right] \left. \right\} \quad - 17 - \quad (\text{B.9})
\end{aligned}$$

$$\begin{aligned}
\tilde{B}_{2h}^{4,2,c} = & \frac{\sin^2 \theta_{12}}{18018\sqrt{5}(k_1^2 + 2\cos\theta_{12}k_2k_1 + k_2^2)^2} \\
& \left\{ 2P_m(k_1)\lambda^2 k_2^2 (k_1^2 + 2\cos\theta_{12}k_2k_1 + k_2^2)^2 \left[104f(11b + 3f) - \lambda^2 \left[6(143b^2 + 156fb + 45f^2)k_1^2 \right. \right. \right. \\
& + 12(143b^2 + 156fb + 45f^2)\cos\theta_{12}k_2k_1 + (715b^2 + 1066fb + 303f^2)k_2^2 + (1001b^2 + 806fb + 237f^2)\cos 2\theta_{12}k_2^2 \left. \left. \right] \right] \\
& - P_m(k_2)(k_1^2 + 2\cos\theta_{12}k_2k_1 + k_2^2)^2 \left[572f^2(7\cos 2\theta_{12} + 5) - 26\lambda^2 f \left[2(44b + 41f)k_1^2 + (264b + 205f)\cos\theta_{12}k_2k_1 \right. \right. \\
& + 35f\cos 3\theta_{12}k_2k_1 + 5(22b + 15f)k_2^2 + \cos 2\theta_{12}(62fk_1^2 + 7(22b + 15f)k_2^2) \left. \right] + \lambda^4 \left[6f(104b + 101f)k_1^4 \right. \\
& + 3(572b^2 + 2132fb + 1305f^2)k_2^2k_1^2 + 5f \left(63f\cos 4\theta_{12}k_1k_2 + 2\cos 3\theta_{12}(57fk_1^2 + 7(26b + 21f)k_2^2) \right) k_2k_1 \\
& + 2\cos\theta_{12}k_1k_2(3f(624b + 505f)k_1^2 + (1716b^2 + 5330fb + 3045f^2)k_2^2) + 5(143b^2 + 390fb + 210f^2)k_2^4 \\
& \left. \left. \left. + \cos 2\theta_{12}(474f^2k_1^4 + 6f(806b + 645f)k_2^2k_1^2 + 7(143b^2 + 390fb + 210f^2)k_2^4) \right] \right] \\
& - P_m(k_3)k_2^2 \left[572f^2(12k_1^2 + 24\cos\theta_{12}k_2k_1 + 7\cos 2\theta_{12}k_2^2 + 5k_2^2) - 26\lambda^2 f \left[4(22b + 21f)k_1^4 + 7(66b + 41f)k_2^2k_1^2 \right. \right. \\
& + 14(11b + 5f)\cos 3\theta_{12}k_2^3k_1 + 2\cos\theta_{12}k_1k_2(4(55b + 36f)k_1^2 + (319b + 205f)k_2^2) + 5(22b + 15f)k_2^4 \\
& + \cos 2\theta_{12}k_2^2((418b + 217f)k_1^2 + 7(22b + 15f)k_2^2) \left. \right] + \lambda^4 \left[12f(26b + 45f)k_1^6 \right. \\
& + (715b^2 + 1378fb + 606f^2)k_2^2k_1^4 + 3(1287b^2 + 2782fb + 1305f^2)k_2^4k_1^2 + \left(7(143b^2 + 130fb + 45f^2)\cos 4\theta_{12}k_1k_2 \right. \\
& + 2\cos 3\theta_{12}(1001(k_1^2 + k_2^2)b^2 + 26f(33k_1^2 + 70k_2^2)b + 15f^2(19k_1^2 + 49k_2^2)) \left. \right) k_2^3k_1 + 2\cos\theta_{12}k_1k_2(12f(26b + 45f)k_1^4 \\
& +(2431b^2 + 4134fb + 1515f^2)k_2^2k_1^2 + (2431b^2 + 5980fb + 3045f^2)k_2^4) + 5(143b^2 + 390fb + 210f^2)k_2^6 \\
& + \cos 2\theta_{12}k_2^2 \left((1001b^2 + 806fb + 474f^2)k_1^4 + 2(2717b^2 + 4888fb + 1935f^2)k_2^2k_1^2 \right. \\
& \left. \left. \left. + 7(143b^2 + 390fb + 210f^2)k_2^4 \right) \right] \right\} \quad (B.10)
\end{aligned}$$

$$\begin{aligned}
\tilde{B}_{2h}^{4,3,s} = & \frac{\sqrt{2} \sin^3 \theta_{12}}{1287 \sqrt{35} (k_1^2 + 2k_2 k_1 \cos \theta_{12} + k_2^2)^2} \\
& \left\{ P_m(k_1) k_2^3 \lambda^4 (143b^2 + 78bf + 15f^2) (k_1 + 2k_2 \cos \theta_{12}) (k_1^2 + 2k_2 k_1 \cos \theta_{12} + k_2^2)^2 \right. \\
& + P_m(k_2) (k_1^2 + 2k_2 k_1 \cos \theta_{12} + k_2^2)^2 \left[572f^2 \cos \theta_{12} - 26f \lambda^2 \left[k_1 k_2 (11b + 5f \cos 2\theta_{12} + 10f) \right. \right. \\
& + \cos \theta_{12} (k_2^2 (22b + 15f) + 6fk_1^2) \left. \right] + \lambda^4 \left[k_2^3 k_1 (143b^2 + 10f(26b + 21f) \cos 2\theta_{12} + 520bf + 315f^2) \right. \\
& + k_2^4 (143b^2 + 390bf + 210f^2) \cos \theta_{12} + 6fk_2 k_1^3 (13b + 10f \cos 2\theta_{12} + 15f) \\
& \left. \left. + 18fk_2^2 k_1^2 \cos \theta_{12} (26b + 5f \cos 2\theta_{12} + 20f) + 30f^2 k_1^4 \cos \theta_{12} \right] \right] \\
& + P_m(k_3) k_2^3 \left[572f^2 (k_2 \cos \theta_{12} + k_1) - 26f \lambda^2 \left[k_2 k_1^2 (44b + 21f) \cos \theta_{12} + k_2^2 k_1 (2(11b + 5f) \cos 2\theta_{12} + 33b + 20f) \right. \right. \\
& + k_2^3 (22b + 15f) \cos \theta_{12} + k_1^3 (11b + 6f) \left. \right] + \lambda^4 \left[k_2 k_1^4 (143b^2 + 78bf + 30f^2) \cos \theta_{12} + 2k_2^2 k_1^3 ((143b^2 + 104bf \right. \\
& \left. + 30f^2) \cos 2\theta_{12} + 143b^2 + 169bf + 45f^2) + 2k_2^3 k_1^2 \cos \theta_{12} ((143b^2 + 130bf + 45f^2) \cos 2\theta_{12} \right. \\
& \left. + 286b^2 + 494bf + 180f^2) + k_2^4 k_1 ((286b^2 + 520bf + 210f^2) \cos 2\theta_{12} + 286b^2 + 650bf + 315f^2) \right. \\
& \left. \left. + k_2^5 (143b^2 + 390bf + 210f^2) \cos \theta_{12} + 15f^2 k_1^5 \right] \right] \quad (B.11)
\end{aligned}$$

$$\begin{aligned}
\tilde{B}_{2h}^{4,4,c} = & \frac{\sin^4 \theta_{12}}{2574 \sqrt{35} (k_1^2 + 2k_2 k_1 \cos \theta_{12} + k_2^2)^2} \\
& \left\{ 2P_m(k_1) \lambda^4 k_2^4 (143b^2 + 26bf + 3f^2) (k_1^2 + 2k_2 k_1 \cos \theta_{12} + k_2^2)^2 \right. \\
& + P_m(k_2) (k_1^2 + 2k_2 k_1 \cos \theta_{12} + k_2^2)^2 \left[572f^2 - 26f \lambda^2 \left[k_2^2 (22b + 15f) + 10fk_2 k_1 \cos \theta_{12} + 2fk_1^2 \right] \right. \\
& + \lambda^4 \left[k_2^4 (143b^2 + 390bf + 210f^2) + 6fk_2^2 k_1^2 (26b + 15f \cos 2\theta_{12} + 30f) + 20fk_2^3 k_1 (26b + 21f) \cos \theta_{12} \right. \\
& \left. \left. + 60f^2 k_2 k_1^3 \cos \theta_{12} + 6f^2 k_1^4 \right] \right] \\
& + P_m(k_3) k_2^4 \left[572f^2 - 26f \lambda^2 \left[k_1^2 (22b + 7f) + 4k_2 k_1 (11b + 5f) \cos \theta_{12} + k_2^2 (22b + 15f) \right] \right. \\
& + \lambda^4 \left[4k_2 k_1^3 (143b^2 + 78bf + 15f^2) \cos \theta_{12} + 2k_2^2 k_1^2 ((143b^2 + 130bf + 45f^2) \cos 2\theta_{12} \right. \\
& \left. + 286b^2 + 338bf + 90f^2) + 4k_2^3 k_1 (143b^2 + 260bf + 105f^2) \cos \theta_{12} + k_1^4 (143b^2 + 26bf + 6f^2) \right. \\
& \left. \left. + k_2^4 (143b^2 + 390bf + 210f^2) \right] \right] \quad (B.12)
\end{aligned}$$

$$\begin{aligned}
\tilde{B}_{3h}^{2,1,s} = & \frac{f}{16170\sqrt{3}k_1k_2(k_1^2 + 2\cos\theta_{12}k_2k_1 + k_2^2)^2} \\
& \left\{ -P_m(k_1)P_m(k_2)(k_1^2 + 2\cos\theta_{12}k_2k_1 + k_2^2) \left[f^2(35f + 44)\sin 6\theta_{12}k_1k_2^3 + \sin 5\theta_{12}((462b^2 + 66f(7f + 9)b + f^2(595f + 682))k_1^2 \right. \right. \\
& + f^2(315f + 341))k_1^2 + 7f^2(5f + 11)k_2^2 \Big] k_2^2 + \sin 4\theta_{12}k_1k_2 \left((693(f + 3)b^2 + 198f(7f + 10)b + f^2(595f + 682))k_1^2 \right. \\
& + (231(6f + 13)b^2 + 308f(7f + 9)b + 2f^2(420f + 517))k_2^2 \Big) + \sin 3\theta_{12} \left(7(33(3f + 7)b^2 + 66f(2f + 3)b \right. \\
& + 5f^2(9f + 11))k_1^4 + (2520f^3 + 154(59b + 19)f^2 + 99(3b(35b + 36) + 14b_2)f + 231b(b(14b + 55) + 14b_2))k_2^2k_1^2 \\
& + 7(75f^3 + 11(22b + 9)f^2 + 198b(b + 2)f + 462b^2)k_2^4 \Big) + \sin 2\theta_{12}k_1k_2 \left(2(1120f^3 + 11(434b + 113)f^2 \right. \\
& + 99(10b(7b + 5) + 7b_2)f + 231b(2b(7b + 13) + 7b_2))k_1^2 + (2625f^3 + 22(504b + 145)f^2 \\
& + 1386(b(11b + 10) + b_2)f + 462b(2b(7b + 18) + 7b_2))k_2^2 \Big) + \sin\theta_{12} \left(7(75f^3 + 11(34b + 5)f^2 \right. \\
& + 99b(7b + 2)f + 231b^2(2b + 1))k_1^4 + (2625f^3 + 11(1092b + 307)f^2 + 99(3b(63b + 50) + 14b_2)f \\
& + 1617b(b(6b + 11) + 2b_2))k_2^2k_1^2 + 14(50f^3 + 22(11b + 2)f^2 + 198b(2b + 1)f + 231b^2(b + 1))k_2^4 \Big) \Big] \\
& + 2P_m(k_2)P_m(k_3)k_1(k_1 + 2\cos\theta_{12}k_2)\sin\theta_{12} \left[7(60f^3 + 11(23b + 5)f^2 + 198b(2b + 1)f + 231b^2(b + 1))k_1^4 \right. \\
& + (525f^3 + 77(23b + 5)f^2 + 99(3b(7b + 4) - 28b_2)f + 231b(b(7b + 4) - 28b_2))k_2^2k_1^2 + (33f^2\cos 4\theta_{12}k_2^2 \\
& + (231(3f + 5)b^2 + 66f(7f + 12)b + f^2(105f + 242))\cos 3\theta_{12}k_1k_2 + \cos 2\theta_{12}(7(33(3f + 7)b^2 \\
& + 66f(2f + 3)b + 5f^2(9f + 11))k_1^2 + 2(105f^3 + 22(21b + 8)f^2 + 99(b(7b + 8) - 7b_2)f \\
& + 231b(5b - 7b_2))k_2^2) \Big) k_1^2 + \cos\theta_{12}k_1k_2 \left((1365f^3 + 22(224b + 59)f^2 + 99(63b^2 + 48b - 14b_2)f \right. \\
& + 231b(b(14b + 23) - 14b_2))k_1^2 - 1386b_2(7b + 3f)k_2^2 \Big) - 462b_2(7b + 3f)k_2^4 \Big] \\
& + P_m(k_3)P_m(k_1)k_2^2 \left[(33f^2\sin 6\theta_{12}k_1k_2^2 + \sin 5\theta_{12}(99(7b^2 + 6fb + 2f^2)k_1^2 + 7f^2(5f + 11)k_2^2)k_2 \right. \\
& + \sin 3\theta_{12}k_2 \left((945f^3 + 77(42b + 17)f^2 + 99(b(35b + 52) - 14b_2)f + 3234b(2b - b_2))k_1^2 + 7(75f^3 + 11(22b + 9)f^2 \right. \\
& + 198b(b + 2)f + 462b^2)k_2^2 \Big) + \sin 2\theta_{12}k_1 \left(2(245f^3 + 110(7b + 2)f^2 + 99(b(7b + 8) - 21b_2)f + 231b(4b - 21b_2))k_1^2 \right. \\
& + (2100f^3 + 11(686b + 193)f^2 + 1386(6b(b + 1) - b_2)f + 462b(b(7b + 20) - 7b_2))k_2^2 \Big) + \sin 4\theta_{12}k_1(33(21b^2 \\
& + 18fb + 5f^2)k_1^2 + (693(2f + 5)b^2 + 308f(4f + 9)b + 2f^2(210f + 407))k_2^2) \Big) k_2 + \sin\theta_{12} \left(-924(7b \right. \\
& + 3f)b_2k_1^4 + (1575f^3 + 11(448b + 113)f^2 + 99(b(49b + 38) - 42b_2)f + 231b(b(14b + 13) - 42b_2))k_2^2k_1^2 \\
& \left. \left. + 14(50f^3 + 22(11b + 2)f^2 + 198b(2b + 1)f + 231b^2(b + 1))k_2^4 \right) \right] \Big\} \quad (B.13)
\end{aligned}$$

$$\begin{aligned}
\tilde{B}_{3h}^{2,2,c} = & \frac{f \sin^2 \theta_{12}}{8085 \sqrt{3} k_1 k_2 (k_1^2 + 2 \cos \theta_{12} k_2 k_1 + k_2^2)^2} \\
& \left\{ -P_m(k_1) P_m(k_2) (k_1^2 + 2 \cos \theta_{12} k_2 k_1 + k_2^2) \left[k_2 \left(k_1^3 (357 f^3 \right. \right. \right. \\
& + 11(147b + 31)f^2 + 33(b(91b + 50) + 7b_2)f + 231b(b(7b + 19) + 7b_2) \Big) + k_2^2 k_1 \Big(567f^3 + 11(217b + 65)f^2 \\
& + 33(2b(56b + 55) + 7b_2)f + 231b(b(7b + 29) + 7b_2) \Big) + f^2(35f + 44) \cos 4\theta_{12} k_2^2 k_1 + \cos 2\theta_{12} k_1 \Big((693(f + 3)b^2 \\
& + 66f(14f + 17)b + f^2(273f + 275))k_1^2 + (231(6f + 13)b^2 + 22f(77f + 87)b + f^2(518f + 627))k_2^2 \Big) \\
& + \cos 3\theta_{12} k_2 \Big((462b^2 + 462f(f + 1)b + f^2(203f + 209))k_1^2 + 7f^2(5f + 11)k_2^2 \Big) \Big) + \cos \theta_{12} \Big(7(33(3f + 7)b^2 \\
& + 66f(f + 1)b + f^2(15f + 11))k_1^4 + (1092f^3 + 22(203b + 57)f^2 + 231(b(29b + 24) + 2b_2)f + 231b(b(14b + 47) \\
& + 14b_2))k_2^2 k_1^2 + 7(66(3f + 7)b^2 + 88f(2f + 3)b + 5f^2(9f + 11))k_2^4 \Big) \Big] \\
& + P_m(k_2) P_m(k_3) k_1 \left[-462b_2(7b + 3f)k_2^5 + (315f^3 + 11(98b + 19)f^2 + 33(5b(7b + 4) - 91b_2)f \right. \\
& + 231b(4b - 35b_2))k_1^2 k_2^3 + (378f^3 + 55(28b + 5)f^2 + 33(56b^2 + 34b - 7b_2)f + 231b(9b - 7b_2))k_1^4 k_2 \\
& + k_1 \left(k_1 k_2 \left(33f^2 \cos 4\theta_{12} k_2^2 + \cos 3\theta_{12} k_1 k_2 (231(3f + 5)b^2 + 66f(7f + 9)b + f^2(105f + 176)) \right) \right. \\
& + 2 \cos 2\theta_{12} \left(231(3(f + 2)k_1^2 + (3f + 5)k_2^2)b^2 + 33(2f(7f + 9)(k_1^2 + k_2^2) - 49b_2 k_2^2)b \right. \\
& \left. \left. + f(f(21f + 22)(6k_1^2 + 5k_2^2) - 693b_2 k_2^2) \right) \right) + \cos \theta_{12} \left(7(33(3f + 7)b^2 + 66f(f + 1)b + f^2(15f + 11))k_1^4 \right. \\
& \left. + (945f^3 + 22(161b + 34)f^2 + 33(b(133b + 94) - 56b_2)f + 231b(23b - 28b_2))k_2^2 k_1^2 - 1386b_2(7b + 3f)k_2^4 \right) \Big] \\
& + P_m(k_3) P_m(k_1) k_2^3 \left[k_1^3 \left(35f^3 + 11(7b + 4)f^2 - 33(b(7b - 8) + 7b_2)f - 231b(b(7b - 4) + 7b_2) \right) \right. \\
& + k_2^2 k_1 \left(378f^3 + 11(119b + 40)f^2 + 33(2b(7b + 29) - 7b_2)f - 231b(b(7b - 13) + 7b_2) \right) \\
& + 33f^2 \cos 4\theta_{12} k_2^2 k_1 + \cos 2\theta_{12} k_1 \left(33k_1^2(21b^2 + 6fb + f^2) + k_2^2(693(2f + 5)b^2 + 22f(35f + 81)b \right. \\
& \left. + f^2(252f + 451)) \right) + \cos 3\theta_{12} k_2 \left(99(7b^2 + 4fb + f^2)k_1^2 + 7f^2(5f + 11)k_2^2 \right) \\
& + \cos \theta_{12} k_2 \left(k_1^2 \left(315f^3 + 44(21b + 10)f^2 + 33(b(7b + 58) - 14b_2)f - 462b(b(7b - 9) + 7b_2) \right) \right. \\
& \left. + 7k_2^2 \left(66(3f + 7)b^2 + 88f(2f + 3)b + 5f^2(9f + 11) \right) \right) \Big] \Big\} \quad (B.14)
\end{aligned}$$

$$\begin{aligned}
\tilde{B}_{3h}^{4,1,s} = & \frac{f^2}{252252\sqrt{10}k_1k_2(k_1^2 + 2\cos\theta_{12}k_2k_1 + k_2^2)^2} \\
& \left\{ -P_m(k_1)P_m(k_2)(k_1^2 + 2\cos\theta_{12}k_2k_1 + k_2^2) \left[(91b(35f + 44) + 2f(1155f + 962))\sin 6\theta_{12}k_1k_2^3 \right. \right. \\
& + \sin 5\theta_{12}k_2^2 \left((11970f^2 + 13(1799b + 727)f + 143b(98b + 125))k_1^2 + 7(91b(5f + 11) + f(330f + 481))k_2^2 \right) \\
& + \sin 4\theta_{12}k_1k_2 \left((29029b^2 + 247(168f + 121)b + f(17955f + 14807))k_1^2 + 13(1890f^2 + (4802b + 1903)f \right. \\
& \left. \left. + 77b(44b + 51))k_2^2 \right) + \sin 2\theta_{12}k_1k_2 \left(26(4543b^2 + (5768f + 3861)b + f(1785f + 1661) + 616b_2)k_1^2 \right. \\
& \left. + (49770f^2 + 13(12061b + 3590)f + 2002(60b^2 + 55b + 8b_2))k_2^2 \right) + \sin\theta_{12} \left(7(5005b^2 + 286(19f + 8)b + 5f(297f \right. \\
& \left. + 208))k_1^4 + (47565f^2 + 26(5992b + 1847)f + 143(b(875b + 794) + 112b_2))k_2^2k_1^2 + 14(675f^2 + 13(149b + 43)f \right. \\
& \left. + 143b(11b + 9))k_2^4 \right) + \sin 3\theta_{12} \left(7(2145b^2 + 26(117f + 88)b + 5f(237f + 208))k_1^4 + (58275f^2 + 91(1881b + 611)f \right. \\
& \left. + 143(b(889b + 871) + 112b_2))k_2^2k_1^2 + 7(1800f^2 + 39(143b + 41)f + 715b(6b + 5))k_2^4 \right) \Big] \\
& + 2P_m(k_2)P_m(k_3)k_1(k_1 + 2\cos\theta_{12}k_2)\sin\theta_{12} \left[7(3575b^2 + 26(163f + 88)b + 5f(267f + 208))k_1^4 + (7455f^2 \right. \\
& \left. + 1183(17b + 5)f + 143(b(70b + 103) - 126b_2))k_2^2k_1^2 + k_1k_2 \left(\cos 4\theta_{12}k_1k_2(455b(7f + 11) + 3f(245f + 481)) \right. \right. \\
& \left. \left. + \cos 3\theta_{12}((6195f^2 + 13(1554b + 499)f + 143b(105b + 113))k_1^2 - 14014b_2k_2^2) \right) + \cos\theta_{12}k_1k_2 \left((29085f^2 \right. \right. \\
& \left. \left. + 13(6286b + 1741)f + 715b(91b + 67) - 16016b_2)k_1^2 - 34034b_2k_2^2 \right) - 2002b_2k_2^4 + \cos 2\theta_{12} \left(7k_1^4(2145b^2 + 26(117f \right. \right. \\
& \left. \left. + 88)b + 5f(237f + 208)) + 2k_2^2k_1^2(4725f^2 + 13(1064b + 277)f + 143(b(105b + 43) - 105b_2)) - 14014b_2k_2^4 \right) \Big] \\
& + P_m(k_3)P_m(k_1)k_2^2 \left[k_2 \left(39(77b + 37f)\sin 6\theta_{12}k_1k_2^2 + \sin 3\theta_{12}k_2 \left(k_1^2(24885f^2 + 91(714b + 269)f \right. \right. \right. \\
& \left. \left. \left. + 143(b(231b + 409) - 112b_2)) \right) + 7k_2^2(1800f^2 + 39(143b + 41)f + 715b(6b + 5)) \right) \Big] \\
& + \sin 5\theta_{12}k_2 \left(39(253b + 117f)k_1^2 + 7(91b(5f + 11) + f(330f + 481))k_2^2 \right) \\
& + \sin 2\theta_{12}k_1 \left(16(735f^2 + 260(7b + 2)f + 143(b(7b + 8) - 21b_2))k_1^2 + (41580f^2 + 13(9212b + 2521)f \right. \\
& \left. + 1001(96b^2 + 69b - 16b_2))k_2^2 \right) + \sin 4\theta_{12}k_1 \left(624(11b + 5f)k_1^2 + (16016b^2 \right. \\
& \left. + 91(382f + 451)b + f(14490f + 17849))k_2^2 \right) + \sin\theta_{12} \left(-32032b_2k_1^4 + (31185f^2 + 26(3143b + 778)f \right. \\
& \left. + 1573b(49b + 20) - 48048b_2)k_2^2k_1^2 + 14(675f^2 + 13(\bar{22}\bar{149}\bar{b} + 43)f + 143b(11b + 9))k_2^4 \right) \Big] \quad (B.15)
\end{aligned}$$

$$\begin{aligned}
\tilde{B}_{3h}^{4,2,c} = & \frac{f^2 \sin^2 \theta_{12}}{126126\sqrt{5}k_1 k_2 (k_1^2 + 2 \cos \theta_{12} k_2 k_1 + k_2^2)^2} \\
& \left\{ -P_m(k_1) P_m(k_2) (k_1^2 + 2 \cos \theta_{12} k_2 k_1 + k_2^2) \left[k_2 \left(2k_1^3 (6132f^2 + 39(539b + 124)f + 143(b(133b + 100) + 14b_2)) \right. \right. \right. \\
& + k_2^2 k_1 (19089f^2 + 13(4669b + 1448)f + 286(b(175b + 164) + 14b_2)) + \cos 4\theta_{12} k_2^2 k_1 (91b(35f + 44) \\
& + f(1995f + 1612)) + 2k_1 \cos 2\theta_{12} \left((5208f^2 + 195(77b + 20)f + 143b(91b + 68)) k_1^2 \right. \\
& \left. \left. \left. + (9618f^2 + 39(665b + 242)f + 143b(133b + 158)) k_2^2 \right) + \cos 3\theta_{12} k_2 \left((14014b^2 \right. \right. \\
& + 91(221f + 165)b + f(8631f + 6565)) k_1^2 + 7(91b(5f + 11) + f(285f + 403)) k_2^2 \right) \right] \\
& + \cos \theta_{12} \left(28(135f^2 + 78(6b + 1)f + 143b(3b + 2)) k_1^4 + (37989f^2 + 13(9205b + 2687)f \right. \\
& \left. + 1001(b(102b + 89) + 8b_2)) k_2^2 k_1^2 + 7(1515f^2 + 13(349b + 113)f + 143b(24b + 25)) k_2^4 \right) \\
& + P_m(k_2) P_m(k_3) k_1 \left[k_2 \left(2(6363f^2 + 39(511b + 100)f + 286(56b^2 + 34b - 7b_2)) k_1^4 + (9135f^2 + 13(2009b + 421)f \right. \right. \\
& + 143(b(140b + 87) - 266b_2)) k_2^2 k_1^2 + k_1 k_2 \left(k_1 k_2 \cos 4\theta_{12} (455b(7f + 11) + 3f(245f + 403)) \right. \\
& \left. \left. + \cos 3\theta_{12} ((5985f^2 + 13(1547b + 433)f + 143b(84b + 121)) k_1^2 - 14014b_2 k_2^2) \right) \right. \\
& \left. - 10010b_2 k_2^4 + 2 \cos 2\theta_{12} \left(3k_1^4 (1659f^2 + 13(385b + 96)f + 572b(7b + 6)) + k_2^2 k_1^2 (4515f^2 + 13741bf \right. \right. \\
& \left. \left. + 429b(28b + 17) + 247(13f - 77b_2)) - 7007b_2 k_2^4 \right) \right] + \cos \theta_{12} k_1 \left(28k_1^4 (135f^2 + 78(6b + 1)f \right. \\
& \left. + 143b(3b + 2)) + k_2^2 k_1^2 (31815f^2 + 13(7189b + 1583)f + 143(b(532b + 327) - 224b_2)) - 58058b_2 k_2^4 \right) \\
& + P_m(k_3) P_m(k_1) k_2^3 \left[4(315f^2 + 78(7b + 4)f - 143(b(7b - 8) + 7b_2)) k_1^3 + (12726f^2 \right. \\
& \left. + 65(532b + 185)f + 143(b(154b + 197) - 28b_2)) k_2^2 k_1 + 39(77b + 31f) \cos 4\theta_{12} k_2^2 k_1 \right. \\
& \left. + 2 \cos 2\theta_{12} k_1 (156(11b + 3f) k_1^2 + (4977f^2 + 13(938b + 499)f + 715b(7b + 23)) k_2^2) \right) \\
& \left. + \cos \theta_{12} k_2 \left(4(2835f^2 + 312(21b + 10)f + 143(b(7b + 58) - 14b_2)) k_1^2 + 7(1515f^2 + 13(349b + 113)f \right. \right. \\
& \left. \left. + 143b(24b + 25)) k_2^2 \right) + \cos 3\theta_{12} k_2 (312(22b + 9f) k_1^2 + 7(91b(5f + 11) + f(285f + 403)) k_2^2) \right] \} \quad (B.16)
\end{aligned}$$

$$\begin{aligned}
\tilde{B}_{3h}^{4,3,s} = & \frac{f^2 \sin^3 \theta_{12}}{9009 \sqrt{70} k_1 k_2 (k_1^2 + 2 \cos \theta_{12} k_2 k_1 + k_2^2)^2} \\
& \left\{ P_m(k_1) P_m(k_2) (k_1^2 + 2 k_2 k_1 \cos \theta_{12} + k_2^2) \left[7 k_1^4 (143 b^2 + 78 b f + 15 f^2) + 2 k_2 \left(k_2 \left(\cos 2 \theta_{12} \left(k_1^2 (13 (161 b + 33) f + 143 b (14 b + 11) + 630 f^2) + 7 k_2^2 (13 b (5 f + 11) + 3 f (10 f + 13)) \right) + k_1 k_2 \cos 3 \theta_{12} (13 b (35 f + 44) + 6 f (35 f + 26)) \right) + k_1 \cos \theta_{12} \left(7 k_1^2 (39 (8 b + 1) f + 143 b (3 b + 1) + 75 f^2) + k_2^2 (13 (343 b + 93) f + 143 b (28 b + 31) + 1260 f^2) \right) + k_2^2 k_1^2 (442 (14 b + 3) f + 143 b (49 b + 34) + 1575 f^2) + 14 k_2^4 (13 (13 b + 3) f + 143 b (b + 1) + 45 f^2) \right] \right. \\
& - P_m(k_2) P_m(k_3) k_1 (k_1 + 2 k_2 \cos \theta_{12}) \left[7 k_1^4 (143 b^2 + 78 b f + 15 f^2) + 2 k_2 k_1 \left(7 \cos \theta_{12} \left(k_1^2 (39 (6 b + 1) f + 143 b (b + 1) + 75 f^2) - 286 b_2 k_2^2 \right) + k_1 k_2 \cos 2 \theta_{12} (65 b (7 f + 11) + 3 f (35 f + 39)) \right) + 2 k_2^2 k_1^2 (13 (91 b + 12) f + 143 (b (7 b + 2) - 7 b_2) + 420 f^2) - 2002 b_2 k_2^4 \right] \\
& - P_m(k_3) P_m(k_1) k_2^4 \left[k_1^2 \left(78 (7 b + 4) f - 143 b (7 b - 8) + 315 f^2 \right) + 14 k_2^2 (13 (13 b + 3) f + 143 b (b + 1) + 45 f^2) + 36 \cos \theta_{12} k_1 k_2 \left(13 b (7 f + 11) + f (35 f + 39) \right) + 78 \cos 3 \theta_{12} k_2 k_1 (11 b + 3 f) + \cos 2 \theta_{12} \left(78 k_1^2 (11 b + 3 f) + 14 k_2^2 (13 b (5 f + 11) + 3 f (10 f + 13)) \right) \right] \left. \right\} \quad (\text{B.17})
\end{aligned}$$

$$\begin{aligned}
\tilde{B}_{3h}^{4,4,c} = & \frac{f^2 \sin^4 \theta_{12}}{9009 \sqrt{35} k_1 (k_1^2 + 2 \cos \theta_{12} k_2 k_1 + k_2^2)^2} \\
& \left\{ P_m(k_1) P_m(k_2) (k_1^2 + 2 k_2 k_1 \cos \theta_{12} + k_2^2) \left[7 k_1^3 (143 b^2 + 39 b f + 6 f^2) + k_2 \cos \theta_{12} \left(7 k_1^2 (286 b^2 + 143 b (f + 1) + f (27 f + 13)) + 2 k_1 k_2 \cos \theta_{12} (13 b (35 f + 44) + f (105 f + 52)) + 7 k_2^2 (13 b (5 f + 11) + f (15 f + 13)) \right) + k_2^2 k_1 \left(39 (7 b + 2) f + 143 b (7 b + 6) + 42 f^2 \right) \right] \right. \\
& - P_m(k_2) P_m(k_3) k_1 \left[k_1 k_2 \left(k_1 k_2 \cos 2 \theta_{12} (65 b (7 f + 11) + 3 f (35 f + 13)) + 7 \cos \theta_{12} \left(k_1^2 (143 b (f + 1) + f (45 f + 13)) - 286 b_2 k_2^2 \right) \right) + k_2^2 k_1^2 (26 b (21 f + 11) - 1001 b_2 + 2 f (105 f + 26)) + 21 k_1^4 f (13 b + 3 f) - 1001 b_2 k_2^4 \right] \\
& - P_m(k_3) P_m(k_1) k_2^4 \left[k_1 \left(39 (11 b + f) \cos 2 \theta_{12} + 26 (7 b + 2) f + 143 b (4 - 7 b) + 63 f^2 \right) - 24 - \right. \\
& \left. + 7 k_2 \cos \theta_{12} \left(13 b (5 f + 11) + f (15 f + 13) \right) \right] \left. \right\} \quad (\text{B.18})
\end{aligned}$$

References

- [1] Planck Collaboration XVII: P. A. R. Ade et al., *Astron. Astrophys.* **594** A17 (2016)
- [2] T. Nishimichi et al., *Publ. Astron. Soc. Jpn.* **59** 1049 (2007)
- [3] F. Bernardeau, S. Colombi, E. Gaztanaga, R. Scoccimarro, *Phys. Rep.* **367** 1 (2002)
- [4] N. Bartolo, S. Matarrese, A. Riotto, *J. Cosmol. Astropart. Phys.* 10(2005)010
- [5] S. Yokoyama, T. Matsubara, A. Taruya, *Phys. Rev. D* **89** 043524 (2014)
- [6] R. Scoccimarro, *Astrophys. J.* **544** 597 (2000)
- [7] P. J. E. Peebles, E. J. Groth, *Astrophys. J.* **196** 1 (1975)
- [8] E. J. Groth, P. J. E. Peebles, *Astrophys. J.* **217** 385 (1977)
- [9] I. Kayo, et al., *Publ. Astron. Soc. Jpn.* **56** 415 (2004)
- [10] E. Gaztanaga, P. Norberg, C. M. Baugh, D. J. Croton, *Mon. Not. Roy. Astron. Soc.* **364** 620 (2005)
- [11] R. C. Nichol, et al., *Mon. Not. Roy. Astron. Soc.* **368** 1507 (2006)
- [12] G. V. Kulkarni, R. C. Nichol, R. K. Sheth, H.-J. Seo, D. J. Eisenstein, A. Gray, *Mon. Not. Roy. Astron. Soc.* **378** 1196 (2007)
- [13] E. Gaztanaga, A. Cabre, F. Castander, M. Crocce, P. Fosalba, *Mon. Not. Roy. Astron. Soc.* **399** 801 (2009)
- [14] C. K. McBride, et al. *Astrophys. J.* **726** 13 (2011)
- [15] C. K. McBride, et al. *Astrophys. J.* **739** 85 (2011)
- [16] F. A. Marin, *Astrophys. J.* **737** 97 (2011)
- [17] F. A. Marin, et al., *Mon. Not. Roy. Astron. Soc.* **432** 2654 (2013)
- [18] H. Guo, C. Li, Y. P. Jing, G. Borner, *Astrophys. J.* **780** 139 (2014)
- [19] H. Guo, et al., *Mon. Not. Roy. Astron. Soc.* **446** 578 (2015)
- [20] P. Gagrani, L. Samushia, *Mon. Not. Roy. Astron. Soc.* **467** 928 (2017)
- [21] D. W. Pearson, L. Samushia, arXiv:1712.04970
- [22] Z. Slepian Z., D. J. Eisenstein, *Mon. Not. Roy. Astron. Soc.* **454** 4142 (2015)
- [23] Z. Slepian Z., D. J. Eisenstein, *Mon. Not. Roy. Astron. Soc.* **455** L31 (2016)
- [24] Z. Slepian, et al., *Mon. Not. Roy. Astron. Soc.* **468** 1070 (2017)
- [25] Z. Slepian, et al., *Mon. Not. Roy. Astron. Soc.* **469** 1738 (2017)
- [26] Z. Slepian Z., D. J. Eisenstein, arXiv:1709.10150
- [27] J. N. Fry, M. Seldner, *Astrophys. J.* **259** 474 (1982)
- [28] R. Scoccimarro, H. A. Feldman, J. N. Fry, J. A. Frieman, *Astrophys. J.* **546** 652 (2001)
- [29] H. A. Feldman, J. A. Frieman, J. N. Fry, R. Scoccimarro, *Phys. Rev. Lett.* **86** 1434 (2001)
- [30] L. Verde, et al., *Mon. Not. Roy. Astron. Soc.* **335** 432 (2002)
- [31] H. Gil-Marín et al., *Mon. Not. R. Astron. Soc.* **451** 539 (2015)
- [32] H. Gil-Marín et al., *Mon. Not. R. Astron. Soc.* **452** 1914 (2015)
- [33] I. Hashimoto, Y. Rasera, A. Taruya, *Phys. Rev. D* **96** 043526 (2017)

- [34] N. Sugiyama, S. Saito, F. Beutler, H-J. Seo, arXiv:1803.02132
- [35] N. Kaiser, *Mon. Not. R. Astron. Soc.* **227** 1 (1987)
- [36] A. J. S. Hamilton, *Astrophys. J.* **385** L5 (1992)
- [37] J. C. Jackson, *Mon. Not. R. Astron. Soc.* **156** 1 (1972)
- [38] J. A. Peacock, S. J. Dodds, *Mon. Not. R. Astron. Soc.* **280** L19 (1996)
- [39] R. Scoccimarro, H. M. P. Couchman, J. A. Frieman, *Astrophys. J.* **517** 531 (1999)
- [40] K. Yamamoto, Y. Nan, C. Hikage, *Phys. Rev. D* **95** 043528 (2017)
- [41] R. Scoccimarro, *Phys. Rev. D* **92** 083532 (2015)
- [42] A. Shirata, Y. Suto, C. Hikage, T. Shiromizu, N. Yoshida, *Phys. Rev. D* **76** 044026 (2007)
- [43] K. Koyama, A. Taruya, T. Hiramatsu, *Phys. Rev. D* **79** 123512 (2009)
- [44] A. Barreira, B. Li, W. Hellwing, C. M. Baugh, S. Pascoli, *J. Cosmol. Astropart. Phys.* 10(2013)027
- [45] E. Bellini, N. Bartolo, S. Matarrese, *J. Cosmol. Astropart. Phys.* 1206(2012)019
- [46] N. Bartolo, E. Bellini, D. Bertacca, S. Matarrese, *J. Cosmol. Astropart. Phys.* 03(2013)034
- [47] Y. Takushima, A. Terukina, K. Yamamoto, *Phys. Rev. D* **89** 104007 (2014)
- [48] Y. Takushima, A. Terukina, K. Yamamoto, *Phys. Rev. D* **92** 104033 (2015)
- [49] D. Munshi, P. Coles, arXiv:1608.04345
- [50] D. Yamauchi, S. Yokoyama, H. Tashiro, *Phys. Rev. D* **96** 123516 (2017)
- [51] S. Hirano, T. Kobayashi, H. Tashiro, S. Yokoyama, arXiv:1801.07885
- [52] A. Raccanelli, D. Bertacca, O. Dore, R. Maartens, *J. Cosmol. Astropart. Phys.* 08(2014)022
- [53] O. Umeh, S. Jolicoeur, R. Maartens, C. Clarkson, *J. Cosmol. Astropart. Phys.* 03(2017)034
- [54] S. Jolicoeur, O. Umeh, R. Maartens, C. Clarkson, *J. Cosmol. Astropart. Phys.* 09(2017)040
- [55] S. Jolicoeur, O. Umeh, R. Maartens, C. Clarkson, *J. Cosmol. Astropart. Phys.* 03(2018)036
- [56] E. Di Dio, H. Perrier, R. Durrer, G. Marozzi, A. Moradinezhad Dizgah, J. Norena, A. Riotto, *J. Cosmology and Astropart. Phys.* 03(2017)006
- [57] E. Di Dio, R. Durrer, G. Marozzi, F. Montanari, *J. Cosmol. Astropart. Phys.* 01(2016)016
- [58] D. Bertacca, A. Raccanelli, N. Bartolo, M. Liguori, S. Matarrese, L. Verde, Licia *Phys. Rev. D* **97** 023531 (2018)
- [59] M. White, *Mon. Not. R. Astron. Soc.* **321** 1 (2001)
- [60] U. Seljak, *Mon. Not. R. Astron. Soc.* **325** 1359 (2001)
- [61] R. Scoccimarro, R. K. Sheth, L. Hui, B. Jain, *Astrophys. J.* **546** 20 (2001)
- [62] A. Cooray, R. Sheth, *Phys. Rep.* **372** 1 (2002)
- [63] C. Hikage, K. Yamamoto, *J. Cosmol. Astropart. Phys.* 2013(08)19
- [64] J. K. Parejko et al., *Mon. Not. R. Astron. Soc.* **429** 98 (2013)
- [65] R. E. Smith, R. K. Sheth, R. Scoccimarro, *Phys. Rev. D* **78** 3523 (2008)
- [66] J. F. Navarro, C. S. Frenk, S. D. M. White, *Astrophys. J.* **490** 493 (1997)
- [67] R. K. Sheth, G. Tormen, *Mon. Not. R. Astron. Soc.* **308** 119 (1999)
- [68] R. K. Sheth, G. Tormen, *Mon. Not. R. Astron. Soc.* **329** 61 (2002)
- [69] H. Parkinson, S. Cole, J. Helly, *Mon. Not. R. Astron. Soc.* **383** 557 (2008)

- [70] T. Kanemaru et al., *Phys. Rev. D* **92** 023523 (2015)
- [71] B. A. Reid, D. N. Spergel, *Astrophys. J.* **698** 143 (2009)
- [72] E. L. Lokas, G. A. Mamon, *Mon. Not. R. Astron. Soc.* **321** 155 (2001)
- [73] Z. Zheng et al., *Astrophys. J.* **633** 791 (2005)
- [74] J. Tinker et al., *Astrophys. J.* **724** 878 (2010)
- [75] V. Springel, *Mon. Not. R. Astron. Soc.* **364** 1105 (2005)
- [76] M. Crocce, S. Pueblas, R. Scoccimarro *Mon. Not. R. Astron. Soc.* **373** 369 (2006)